



Research and application of a hybrid forecasting framework based on multi-objective optimization for electrical power system

Jianzhou Wang ^a, Wendong Yang ^{a,*}, Pei Du ^a, Yifan Li ^b

^a School of Statistics, Dongbei University of Finance and Economics, Dalian, 116025, China

^b College of Letters and Science, University of California-Los Angeles, Los Angeles, CA, 90024, USA



ARTICLE INFO

Article history:

Received 18 April 2017

Received in revised form

20 January 2018

Accepted 23 January 2018

Available online 3 February 2018

Keywords:

Electrical power system

Hybrid forecasting framework

Multi-objective optimization algorithm

Forecasting accuracy and stability

ABSTRACT

Electrical power system (EPS) forecasting plays a significant role in economic and social development but it remains an extremely challenging task. Because of its significance, relevant studies on EPS are especially needed. More specifically, only a few of the previous studies in this area conducted in-depth investigations of the entire EPS forecasting and merely focused on modeling individual signals centered on wind speed or electrical load. Moreover, most of these past studies concentrated on accuracy improvements and usually ignore the significance of forecasting stability. Therefore, to simultaneously achieve high accuracy and dependable stability, a hybrid forecasting framework based on the multi-objective dragonfly algorithm (MODA) was successfully developed in this study. The framework consists of four modules—data preprocessing, optimization, forecasting, and evaluation modules. In this framework, MODA is employed to optimize the Elman neural network (ENN) model as a part of the optimization module to overcome the drawbacks of single-objective optimization algorithms. In addition, data preprocessing and evaluation modules are incorporated to improve forecasting performance and conduct a comprehensive evaluation for this framework, respectively. Empirical results reveal that the developed forecasting framework can be an effective tool for the planning and management of power grids.

© 2018 Elsevier Ltd. All rights reserved.

1. Introduction

The power industry is an important basic industry needed for national economic and social developments. Moreover, electrical safety affects the overall state of economic development, sustained harmony in society, lives of the common people, and security of property. As most people are aware of, the electrical power system (EPS) is a complex system—which simultaneously accomplishes generation, transmission, distribution, and sale of electric energy—playing an important role in social and economic developments. Furthermore, the control provided by EPS contributes to the orderly management of electricity and reasonable operational plans, energy and cost saving, and substantial economic and social benefits [1]. Hence, researches that focus on EPS have immense political and economic importance for the whole society.

Many studies related to EPS have been conducted, namely dynamic operation and control strategies for microgrid hybrid power systems [2], connection decisions of distribution transformers [3], forecasting issues including electricity load forecasting [4], wind power forecasting [5], wind speed forecasting [6], solar radiation forecasting [7], output power of photovoltaic plants [8], and so on. In general, many problems still exist in the hybrid generation system, and researchers have made in-depth exploration and analysis focusing on unsymmetrical faults [9], microgrid distribution ground fault [10], and unbalanced distribution network fault [11], etc. For instance, Qu et al. [12] proposed a novel intelligent damping controller to reduce power fluctuations, voltage support and damping in hybrid power multi-systems. The EPS forecasting is a very promising area in hybrid power system, which also plays a significant role in the operation of hybrid power systems. However, it remains an extremely challenging task. Therefore, this study focuses on the forecasting issues with the goal of developing an effective forecasting framework.

There are three main signals connected to generation,

* Corresponding author. School of Statistics, Dongbei University of Finance and Economics, Dalian, Liaoning, 116025, China.

E-mail address: hshwendong@hotmail.com (W. Yang).

List of abbreviations	
EPS	Electrical power system
ARMA	Autoregressive moving average process
ARIMA	Autoregressive integrated moving average
NWP	Numerical weather prediction
DFS	Date-framework strategy
MERRA	Modern-era retrospective analysis for research and applications
WIND Toolkit	Wind integration national dataset Toolkit
IEAM	Improved environment adaptation method
AnEn	Analog ensemble
AI	Artificial intelligence
ANN	Artificial neural network
GPR	Gaussian process regression
RFNN	Random fuzzy neural networks
MLP	Multi-layered perceptron
ELM	Extreme learning machine
KELM	Kernel extreme learning machine
GRNN	Generalized regression neural network
ENN	Elman neural network
BPNN	Back propagation neural network
SVM	Support vector machine
SVR	Support vector regression
LSSVM	Least square support vector machine
GNM	Generalized neuron model
NSW	New south wales
SG	Singapore
WT	Wavelet transform
PMSC	Permanent magnet synchronous generator
EMD	Empirical mode decomposition
EEMD	Ensemble empirical mode decomposition
CEEMDAN	Complete ensemble empirical mode decomposition with adaptive noise
ICEEMDAN	Improved complete ensemble empirical mode decomposition with adaptive noise
IMFs	Intrinsic mode functions
PSO	Particle swarm optimization
GABICS	Genetic algorithm binary improved cuckoo search
CS	Cuckoo search
SAPSO	Self-adaptive particle swarm optimization
DA	Dragonfly algorithm
BDA	Binary dragonfly algorithm
MODA	Multi-objective dragonfly algorithm
MOPSO	Multi-objective particle swarm optimization
DM	Diebold-Mariano
FE	Forecasting effectiveness
AE	Average error
MAE	Mean absolute error
RMSE	Root mean square error
NMSE	Normalized mean square error
MAPE	Mean absolute percentage error
FB	Fractional bias
IA	Index of agreement
TIC	Theil's inequality coefficient
RE	Relative error
RE _{MAPE}	Decreased relative error of MAPE
WTG	Wind turbine generator

distribution, and consumption in the EPS, namely short-term wind speed data, electrical power load data and electricity price data, which are all crucial for planning and managing a power grid [13]. To be specific, firstly, wind energy exhibits the most consistent and rapid deployment of power generating capacities than any other renewable energy resources [14]. In 2015, the global wind power industry reached an annual market growth of 20% with the installation generating units having more than 60 000 MW capacities. In China alone, the total capacity of new installations made by the wind power industry was 30 500 MW. By the end of 2015, the total global capacity reached 432 419 MW, gaining a cumulative growth of 17% [15]. However, the intermittent and stochastic characteristics of wind speed pose many challenges, i.e., the increase of costs and the decrease of reliability and stability of EPS [16]. One way to tackle these challenges is to improve forecasting accuracy for wind speed and wind power [17]. Secondly, the basic information for establishing the scheduling plan and reducing management risk—which is a decisive part of EPS risk management [18]—includes future changes in the power load series. Evidently, if the forecasting accuracy of the electrical power load could be improved, then enormous economic benefits could be achieved [19]. Finally, the cost of electricity is related to the aspects of consumption as these play vital roles in balancing the generation and consumption of electricity. Thus, a highly accurate cost forecasting is of great significance for the whole EPS and electricity market [20].

As discussed above, an effective forecasting method is one of the most crucial tools employed in EPS management [21]. However, despite its significance, relevant research for the whole EPS is still poor. More specifically, most recent analyses are focused on modeling individual signals, with either wind speed or electrical

power load dominating. Therefore, it is quite urgent and necessary to develop a novel and robust forecasting framework for these three key signals of EPS. Depending on the computational principle involved, forecasting algorithms can be classified into four categories: statistical, physical, artificial intelligence, and hybrid algorithms.

Statistical algorithms attempt to find the relationship between past and future values in a time series, and to develop statistical and mathematical models for better real-time forecasting [22]. The forecasting performance of statistical models can be improved under the condition that input variables are convergent in the normal distribution [23]. The typical statistical model, autoregressive integrated moving average (ARIMA), is widely employed in the forecasting fields, such as short-term load forecasting [24], wind speed forecasting [25], electricity demand forecasting [26] and electricity price forecasting [27]. Physical algorithms utilize physical variables, such as temperature and humidity, to achieve time series forecasting [22]. However, the physical model consumes large amounts of computing resources. The numerical weather prediction (NWP) model, acknowledged as one of the most widely used physical forecasting model for wind speed forecasting [28], electricity demand forecasting [29], wind power forecasting [30], and wind resource assessment [31], is designed to solve atmospheric equations and identify atmospheric changes. To the best of the knowledge of the authors, artificial intelligence algorithms have been widely employed in many fields, including electric load forecasting [32,33], wind speed forecasting [34,35], electricity price forecasting [36], assessment of wind resources [37], energy optimization and analysis modeling [38], optimization of transesterification process [39], analysis and forecasting of oil consumption [40] and so on, mainly because of the flexibility,

symbolic reasoning and explanation abilities of these algorithms [41]. Furthermore, artificial intelligence models are considered as one of the powerful methods with fault tolerance and strength to tackle forecasting issues and yield better performance [42]. To further improve forecasting, researchers began to focus on integrating artificial intelligence with new methods to develop strong hybrid algorithms. These methods include grey correlation analysis [43], gaussian process regression [44], date-framework strategy and improved feature selection technology [45], phase space reconstruction [46], wavelet transform [47], improved environment adaptation method [48], and so on. Their studies indicate that a hybrid model that integrates existing approaches can always yield better performance than a single forecasting model [49]. Accordingly, because of its superiority over other models, the application of hybrid forecasting models has become a current trend in time series forecasting. The summary of the reviewed forecasting models is listed in Table 1.

From the review of the abovementioned literature, the following

can be summarized [13,19]: (1) The statistical method is more suitable for linear trends data but unsuitable for data with high noise and fluctuation. In this regard, the data of EPS always show high volatility, irregularity, and other tendencies. Hence, the fatal weakness of statistical methods is, forecasting errors will greatly increase when the environmental or sociological factors suddenly change [50]; (2) Physical forecasting methods perform poorly in short-term forecasting and consume large amounts of computing resources as these are sensitive to market information [51]; (3) Artificial neural networks have relative dependence on data, unstable—which makes determining the network structure difficult—and can easily get trapped in the local minimum. (4) Most recent researches combined with the single-objective optimization algorithm are focused on improving forecasting accuracy but usually ignore the significance of forecasting effectiveness determined by its stability [52]. Therefore, in consideration of high accuracy and stability, the application of multi-objective optimization algorithms in the forecasting fields is worth studying.

Table 1
Summary of reviewed forecasting models.

Models	Variable	Datasets	Results	Ref
Statistical Forecasting models				
ARIMA-based model	Electrical load	Hourly load data of Taipower system in 2007	The forecasting effectiveness of the developed model is superior to compared models.	[24]
ARIMA-ANN	Wind speed	24 hourly mean data for one month in Mexico	The proposed model performs better than the single model in the three areas studied.	[25]
Seasonal ARIMA, residual modification	Electrical load	Data from 2006 to 2010 in northwestern China	The proposed model is superior to the seasonal ARIMA model.	[26]
ARIMA	Electricity price	Hourly Data in Spain and California markets	The proposed model provides reliable and accurate forecasting results.	[27]
Physical Forecasting Models				
Kalman Filter; NWP	Wind speed	Hourly data for Cork Airport in Ireland	The proposed model is effective in wind speed forecasting	[28]
NWP and ARIMA	Electrical load	Daily data from 2003 to 2009 in Italy	Data produced by NWP models can improve forecasting performance especially for the hottest regions.	[29]
NWP and ANN	Wind speed; wind power	Three wind turbines in southern Italy	There is an interesting improvement in forecasting performance.	[30]
MERRA, AnEn based on MERRA and WIND Toolkit	Wind speed	Nine locations in the United States	It gives a general overview of NWP models and how they overcame the inadequacies of classical wind measurements.	[31]
Artificial Intelligent Forecasting Models				
SVR	Electrical load	Electric load data of Northeast China	The proposed model is a promising alternative for electric load forecasting.	[32]
RFNN LSSVM	Electrical load Wind speed	Hourly load data in Macau Data from January 2001 to December 2006 in Mazong Mountain and Jiuquan, China	The model presents a much higher variability. The proposed model is simple and quite efficient.	[33] [34]
BPNN	Wind speed	Three verification units in Penglai, China	The proposed model not only has advantages when compared benchmark models, but also has great potential for application to wind power system.	[35]
MLP	Electricity prices	Data points (2856 in all) in the southern Italy electricity market	The proposed model has a comprehensive operation and high quality in terms of flexibility, which is an effective method for electricity price forecasting.	[36]
Hybrid Forecasting Models				
Grey correlation analysis, SVM, and CS	Wind speed	Wind farm in Peng Lai, China	The hybrid model can improve forecasting accuracy in single WTG.	[43]
ARIMA, ELM, SVM, LSSVM, and GPR	Wind speed	Two wind farms in China	The proposed combination model can yield more accurate and reliable forecasting results.	[44]
GABICS, DFS, and ELM	Date-framework and lag variables	Australian electricity market (half-hourly electricity loads) in 2010 and 2011	The proposed model not only yields an effective features subset but also robust and highly accurate forecasting results.	[45]
SVR-based model	Electrical load	Half-hourly electrical load in New South Wales from May 2–21, 2007	Experimental results demonstrate the computational superiority of the proposed model over the compared models.	[46]
ARMA, SAPSO, KELM, and Wavelet transform	electricity price	Electricity price data from three different markets	The model has a more accurate forecast, better generality, and practicability than individual models and other hybrid models.	[47]
GNM, IEAM, and WT	Electricity price	Electricity price of the New South Wales electricity market	The proposed hybrid forecasting model shows high forecasting accuracy for electricity demand and price.	[48]

In this paper, with the goal of overcoming the above-mentioned problems, a novel robust forecasting framework was successfully developed for a complex EPS, consisting of four modules: data preprocessing, forecasting, optimization, and evaluation modules. In this structure, a hybrid forecasting framework based on Elman neural network (ENN) is developed for EPS, which successfully and effectively overcame the abovementioned limitations. More specifically, the ENN model is employed to improve forecasting performance as part of the basic forecasting module. To further boost forecasting effectiveness, the novel hybrid forecasting framework developed combines the mechanism of “decomposed and reconstructed”, Elman neural network model, and advanced multi-objective optimization algorithms. Firstly, to improve forecasting performance, raw data in the EPS are decomposed using advanced data preprocessing technology, and then the high-frequency signal is removed to guarantee that the main feature can be successfully and effectively identified and extracted; Secondly, the ENN model optimized by the multi-objective intelligence optimization algorithm is used to forecast future changes for the purpose of simultaneously achieving the abovementioned two relatively independent objectives (i.e., high accuracy and stability). Thirdly, the hybrid forecasting framework is used to conduct multi-step forecasting for EPS. Finally, the evaluation module is employed to conduct a comprehensive estimation and to verify the effectiveness of the forecasting framework. Hybridization takes full advantage of the strength of each part and ultimately achieves successful forecasting for the main signals in EPS for the first time. In brief, the main purpose of this study is to provide an effective forecasting technique for the entire EPS and make up for the insufficiency of existing researches so that the framework can be used in real applications. The experimental results show that the developed hybrid forecasting framework has good adaptability for real EPS operations. More specifically, EPS forecasting plays important roles in safety operations, daily distribution, and economics of the system. Moreover, the outstanding forecasting effectiveness of the developed framework is seen to bring enormous benefits in the scheduling of EPS. These benefits include reducing the spinning reserve capacity of thermal power units, saving production costs, avoiding power grid collapse and enhancing the security of EPS, improving economic dispatching, and helping decision-makers establish plans, all of which also provide basic and useful information for planning decisions of electric power companies.

The main contributions of this study are summarized as follows:

- (1) Effective forecasting provides better basis for electrical power grid management and planning. However, despite its importance, few researchers focus on the forecasting model of the whole EPS. Most researchers rather center their attention on modeling individual signals. Therefore, in order to perform multi-step forecasting for complex and crucial EPS, a novel hybrid forecasting framework is successfully developed in this paper. Its effectiveness is well validated in three sites including six datasets, indicating that the developed hybrid forecasting framework is applicable and effective for EPS.
- (2) An original multi-objective optimization algorithm is initially employed to optimize the initial weight and threshold of the ENN model to simultaneously effect high forecasting accuracy and stability. All the while, the data preprocessing module, using the strategy of the “decomposed and reconstructed” theory, effectively eliminates the negative influence of noise and explores the inner characteristics of the original data. These indicate that these modules can effectively boost the performance of the developed forecasting framework.

- (3) An innovative version of fitness functions based on the bias-variance framework are designed to correspond to each objective of the multi-objective optimization issues in the optimization module to evaluate forecasting accuracy and stability.
- (4) A more comprehensive evaluation module of the developed forecasting framework is proposed, including two testing methods and eight typical metric rules. The metric rules, typically used in relevant studies, significantly affects the evaluation of the forecasting performance. More importantly, testing needs to be done to confirm the effectiveness of the forecasting framework from the statistical perspective.

The rest of this paper is organized as follows: The required methods are introduced in Section 2, the developed hybrid forecasting framework is presented in Section 3, the experiments and comparative results are described and discussed in Section 4, insights of the authors on the experimental results are discussed in Section 5, and finally, the conclusions of the study are found in Section 6.

2. Methodology

In this section, the required methods that were applied in the developed forecasting framework are introduced as follows.

2.1. The decomposition approach in data preprocessing

In general, most decomposition approaches perform well only when the signal satisfies certain characteristics. For instance, the wavelet decomposition approach requires non-stationary linear data, whereas the Fourier decomposition approach is mainly used to deal with smooth and cyclic data. The improved complete ensemble empirical mode decomposition with adaptive noise (ICEEMDAN) is a novel decomposition method for data pre-processing developed by Colominas et al. [53] to advance the performance of the empirical mode decomposition (EMD) family. The EMD was developed by Huang et al. [54] and is employed to decompose original signals into some intrinsic mode functions (IMFs). Unfortunately, there are disadvantages in combining the mode with EMD [55]. Therefore, Wu and Huang [56] proposed the ensemble empirical mode decomposition (EEMD) method instead. Although the EEMD achieves pronounced improvements and more stability, it is difficult to entirely neutralize the added noise. To overcome this drawback, the complete ensemble empirical mode decomposition with adaptive noise (CEEMDAN) is developed by Torres et al. [57]. However, CEEMDAN can still be improved because its modes contain some residual noises and the signal information appears “later” than that in EEMD along with some “spurious” modes in the early decomposed stages. To resolve these issues, the improved complete ensemble empirical mode decomposition with adaptive noise (ICEEMDAN) is developed, which can effectively decompose the raw data of EPS, being superiority than other approaches. Details regarding ICEEMDAN are given by Colominas et al. [53].

2.2. Brief overview of multi-objective optimization algorithm

The original swarm intelligence optimization algorithm named dragonfly algorithm (DA), developed by Seyedali Mirjalili [58], is inspired by the behavior of dragonflies in nature. For solving discrete and multi-objective problems, Seyedali Mirjalili also developed the binary and multi-objective versions of DA, i.e., binary dragonfly algorithm (BDA) and multi-objective dragonfly algorithm (MODA). The performances of the proposed algorithms were

evaluated through several test problems and one real case study, and the results reveal that the developed algorithms can effectively solve optimization problems in different fields. In this study, MODA is employed to optimize the ENN model and its description is provided in this section. The detailed description of the DA algorithms can be found in Ref. [58] and its improved versions are be found in Ref. [59].

The objectives of multi-objective optimization problems are usually conflicting. In that regard, the Pareto optimal solutions set provides an answer as it represents the best trade-offs between the different objectives [60]. In general, the multi-objective optimization problem can be expressed as follows.

Minimize:

$$F(\vec{x}) = \{f_1(\vec{x}), f_2(\vec{x}), \dots, f_o(\vec{x})\} \quad (1)$$

Subject to:

$$g_i(\vec{x}) \geq 0, \quad i = 1, 2, \dots, m \quad (2)$$

$$h_i(\vec{x}) \geq 0, \quad i = 1, 2, \dots, p \quad (3)$$

$$L_i \leq x_i \leq U_i, \quad i = 1, 2, \dots, n \quad (4)$$

where o denotes the number of objectives, m is the number of inequality constraints, p is the number of equality constraints, and L_i and U_i are the lower and upper boundaries of the i -th variables, respectively.

Definition 1. Pareto dominance [61]

Suppose that there are two vectors: $\vec{x} = (x_1, x_2, \dots, x_k)$ and $\vec{y} = (y_1, y_2, \dots, y_k)$. Vector x dominates y , denoted as $x > y$, if:

$$\forall i \{1, 2, \dots, k\}, [f(x_i) \geq f(y_i)] \wedge [i \in 1, 2, \dots, k : f(x_i)] \quad (5)$$

Definition 2. Pareto optimality [62]

The solution $\vec{x} \in X$ is named a Pareto optimal if:

$$\nexists \vec{y} \in X | F(\vec{y}) > F(\vec{x}) \quad (6)$$

Two solutions are non-dominated with respect to each other if neither of them dominates the other.

Definition 3. Pareto optimal set

The set including all non-dominated solutions is named Pareto set as follows:

$$P_s := \{x, y \in X | \exists F(y) > F(x)\} \quad (7)$$

Definition 4. Pareto optimal front

A set containing the corresponding values of Pareto optimal solutions in a Pareto optimal set is defined as Pareto optimal front:

$$P_f := \{F(x) | x \in P_s\} \quad (8)$$

For tackling multi-objective optimization problems by the MODA method, an archive is employed to store and retrieve the best approximations of the true Pareto optimal solutions in the optimization process. The position updating of search agents is the same as the DA algorithm while the food sources are chosen from the archive. A food source is selected from the least populated area of the Pareto optimal front to obtain a well-spread front similar to

the multi-objective particle swarm optimization algorithm [63]. The search space is segmented to find the least populated region of the Pareto optimal front. Afterwards, selection using the roulette-wheel mechanism for each segment is conducted. To select enemies from the archive, the worst hyper-sphere should be selected to discourage the dragonflies from searching through non-promising crowded areas. The selection is also done by a roulette-wheel mechanism for each segment. The roulette-wheel mechanism yields high probabilities of obtaining the most crowded hyper-spheres to be chosen as enemies.

In the optimization process, the archive should be updated regularly as it may become full. Hence, a mechanism taken from the studies of Coello et al. [64] is employed to manage the archive. Details regarding MODA are provided in Ref. [58] and its pseudo-code algorithm is presented in Algorithm 1.

Algorithm 1: MODA

Objective functions:

$$\min \begin{cases} \text{fitness}_1 = |\text{Bias}(\hat{x})| \\ \text{fitness}_2 = \text{Std}(x - \hat{x}) \end{cases}$$

Output:

X^* — X with the best fitness

Parameters:

$Iter_{\text{Max}}$ —the maximum iterations

n —the dragonflies' number

F_i —the fitness of i -th dragonfly

$[L_i, U_i]$ —the boundaries of the i -th variable

X_i —the position of i -th dragonfly

ΔX_i —the step vector

t —the current iterations

d —the dimension of the optimized problem.

```

1 /*Set the basic parameters of MODA. */
2 /*Initialize the dragonflies population  $X_i$  ( $i = 1, 2, \dots, n$ ) randomly. */
3 /*Initialize the step vectors  $\Delta X_i$  ( $i = 1, 2, \dots, n$ ). */
4 /*Define the maximum number of hyper spheres (segments). */
5 /*Define the archive size. */
6 FOR EACH  $i: 1 \leq i \leq n$  DO
7   | Calculate the corresponding  $F_i$  using ranking process
8 END FOR
9 /*Determine the best dragonflies and suppose it as the elite. */
10 WHILE ( $t < Iter_{\text{Max}}$ ) DO
11   | /*Calculate the objective values of all dragonflies. */
12   | /*Find the non-dominated solutions. */
13   | /*Update the archive in regard to the obtained non-dominated solutions. */
14   | IF the archive is full DO
15   |   | /*Omit some solutions from the archive to add the new solutions. */
16   | END IF
17   | IF any new added solutions to the archive is outside hyper spheres DO
18   |   | /*Update and re-position all of the hyper to cover the new solutions. */
19   | END IF
20   | Select a food source from archive:  $X^* = \text{SelectFood}(\text{archive})$ 
21   | Select an enemy from archive:  $X = \text{SelectEnemy}(\text{archive})$ 
22   | /*Update the step vectors. */
23   |  $\Delta X_{t+1} = (sS_i + aA_i + cC_i + fF_i + eE_i) + w\Delta X_i$ 
24   | /*Update the position vectors according to different conditions. */
25   |  $X_{t+1} = X_t + \Delta X_{t+1}$ 
26   |  $X_{t+1} = X_t + L\epsilon \text{vy}(d) \times X_t$ 
27 END WHILE
28 RETURN  $X^*$ 

```

2.3. Elman neural network model

The Elman neural network is a simple but well-known recurrent neural network developed by Elman [65]. This type of network consists of three layers—input layer, hidden layer and output layer. Thus, it is similar to a three-layer feed-forward neural network. However, compared with other feed-forward neural networks, the ENN has additional recurrent layers. The special connections—self-connections of the recurrent layers—can make ENN very sensitive to historical data, and this characteristic enhances its ability in handling dynamic information [22]. Moreover, lying between the traditional feed-forward perception and the classic recurrent networks, ENN combines the advantages of both networks. Such a combination has been very widely used in many fields, such as air quality forecasting [66], hybrid power control system [67], and hybrid control of a wind induction generator [68]. Relevant formulas and steps involved in ENN are found in the corresponding literature [69,70].

2.4. Elman neural network optimized by multi-objective optimization algorithm

To overcome the drawbacks of individual algorithms, achieve higher accuracy and stability, and consequently improve forecasting performance, the initial weight and threshold of the ENN is optimized by the novel multi-objective dragonfly algorithm. The corresponding algorithm MODA-ENN is presented in Algorithm 2.

Algorithm 2: MODA-ENN

Objective functions:

$$\min \begin{cases} \text{fitness}_1 = |\text{Bias}(\hat{x})| \\ \text{fitness}_2 = \text{Std}(x - \hat{x}) \end{cases}$$

Input:

$x_t^{(0)} = (x^{(0)}(1), x^{(0)}(2), \dots, x^{(0)}(p))$ —the training data

$x_f^{(0)} = (x^{(0)}(p+1), x^{(0)}(p+2), \dots, x^{(0)}(p+l))$ —the testing data

Output:

$\hat{y}_f^{(0)} = (\hat{y}^{(0)}(p+1), \hat{y}^{(0)}(p+2), \dots, \hat{y}^{(0)}(p+l))$ —the forecasting data

Parameters:

Iter_{Max} —the maximum iterations

n —the dragonflies' number

F_i —the fitness of i -th dragonfly

$[L_i, U_i]$ —the boundaries of the i -th variable

X_i —the position of i -th dragonfly

ΔX_i —the step vector

t —the current iterations

d —the dimension of the optimized problem

```

1 /*Set the basic parameters of MODA. */
2 /*Initialize the dragonflies population  $X_i$  ( $i = 1, 2, \dots, n$ ) randomly. */
3 /*Initialize the step vectors  $\Delta X_i$  ( $i = 1, 2, \dots, n$ ). */
4 /*Define the maximum number of hyper spheres (segments). */
5 /*Define the archive size. */
6 FOR EACH  $i: 1 \leq i \leq n$  DO
7   | Calculate the corresponding  $F_i$  using ranking process
8 END FOR
9 /*Determine the best dragonflies and suppose it as the elite. */
10 WHILE ( $t < \text{Iter}_{\text{Max}}$ ) DO
11   /*Calculate the objective values of all dragonflies. */
12   /*Find the non-dominated solutions. */
13   /*Update the archive in regard to the obtained non-dominated solutions. */
14   IF the archive is full DO
15     | /* Omit some solutions from the archive to add the new solutions. */
16   END IF
17   IF any new added solutions to the archive is outside hyper spheres DO
18     | /* Update and re-position all of the hyper to cover the new solutions. */
19   END IF
20   Select a food source from archive:  $X^* = \text{SelectFood}(\text{archive})$ 
21   Select an enemy from archive:  $X^* = \text{SelectEnemy}(\text{archive})$ 
22   /*Update the step vectors. */
23    $\Delta X_{t+1} = (sS_i + aA_i + cC_i + jF_i + eE_i) + w\Delta X_t$ 
24   /*Update the position vectors according to different conditions. */
25    $X_{t+1} = X_t + \Delta X_{t+1}$ 
26    $X_{t+1} = X_t + \text{Levy}(d) \times X_t$ 
27   Check and correct the new positions based on the boundaries  $[L_i, U_i]$ 
28    $t=t+1$ 
29 END WHILE
30 RETURN  $X^*$ 
31 Set  $X^*$  as the initial weight and threshold of ENN
32 train and update the weight and threshold of ENN
33 Input the historical data into ENN to forecast the future changes  $y_f$ 

```

There are two commonly used criteria for verifying forecasting effectiveness, accuracy and stability. However, most studies in the past are focused on improving only one of the criteria, either forecasting or accuracy, usually ignoring the significance of considering these two criteria simultaneously. Moreover, relevant research is still poor and cannot always satisfy the growing requirements of forecasting effectiveness. Therefore, both objectives—high accuracy and stability—should be studied simultaneously and implemented in the optimization module.

Based on the bias-variance framework [71], the fitness function of the above-mentioned optimization issue is defined in this paper—with both accuracy and stability considered. The decomposition of the bias-variance framework is defined as follows.

$$\begin{aligned}
 \mathbf{E}(\hat{x} - x)^2 &= \mathbf{E}[\hat{x} - \mathbf{E}(\hat{x}) + \mathbf{E}(\hat{x}) - \mathbf{E}(x)]^2 \\
 &= \mathbf{E}[\hat{x} - \mathbf{E}(\hat{x})]^2 + [\mathbf{E}(\hat{x}) - \mathbf{E}(x)]^2 \\
 &= \text{Var}(\hat{x}) + \text{Bias}^2(\hat{x})
 \end{aligned} \tag{9}$$

where x is the actual value, \hat{x} is the forecasted value, and \mathbf{E} is the expectation value of the corresponding variable.

The bias equals the average difference between the actual and forecasted values, which represents forecasting accuracy. A smaller absolute value of the bias represents a more accurate forecasting accuracy. On the other hand, the performance variance can represent forecasting stability. A smaller variance value indicates a more stable forecasting performance. However, in the conduct of most of the experiments, it was found that the criteria are not suitable for

the problems that this study seeks to address. Thus, the standard deviation of the forecasting errors is selected as another fitness function to represent the stability of the model. Therefore, in this paper, the fitness function for accuracy and stability is formulated as follows:

$$\min \begin{cases} \text{fitness}_1 = |\text{Bias}(\hat{x})| \\ \text{fitness}_2 = \text{Std}(x - \hat{x}) \end{cases} \quad (10)$$

3. The hybrid forecasting framework for the electrical power system

In consideration of the drawbacks discussed above, a hybrid forecasting framework based on Elman neural network (ENN) is developed consisting of four modules—data preprocessing, optimization, forecasting, and evaluation modules. The flowchart of the developed hybrid forecasting framework is shown in Fig. 1, which is composed of four parts denoted as A, B, C and D. Part A presents the procedure of the developed hybrid forecasting framework for EPS forecasting, which also is the main procedure of this study. Besides, the other three parts (i.e., part B, C and D) is three most important components in the developed forecasting framework and the details are as follows: part B provides the simple map of the study areas and the decomposed and reconstructed strategy used in the data preprocessing stage, and the optimized ENN model based on multi-objective optimization algorithm is shown in part C, whereas part D denotes the structure of ENN model.

More specifically, in this framework, the ENN model is employed to improve the forecasting performance for electrical

power system. To further boost forecasting effectiveness, a novel hybrid forecasting framework that combines the strategy of the “decomposed and reconstructed”, the Elman neural network model, and the advanced multi-objective optimization algorithms is successfully developed in this paper. The framework is also composed of four steps: First, to eliminate the negative influence of noise and improve forecasting effectiveness, the original time series in EPS are decomposed and reconstructed using the advanced data preprocessing technology in the data preprocessing module, as shown in Fig. 1 part B; Second, the ENN model optimized by the multi-objective dragonfly algorithm is developed to forecast future changes so as to simultaneously achieve high accuracy and stability, which successfully established the forecasting module as shown in Fig. 1 part C; Third, the multi-step forecasting strategy [19] is integrated in the forecasting framework to perform multi-step forecasting for EPS; Finally, the evaluation module is used to verify the forecasting effectiveness of the developed framework. In summary, the useful combination takes full advantage of the merits of each method to ultimately achieve success such that the developed hybrid forecasting framework designed for EPS is found to be not only applicable but also effective.

4. Experiments and analysis

This section provides details of data description, the performance metric, two testing methods and three experiments, and corresponding analysis. Through practical experiments, the goal is to verify the performance of the developed hybrid forecasting framework.

4.1. Data description

There are three main signals connected to generation,

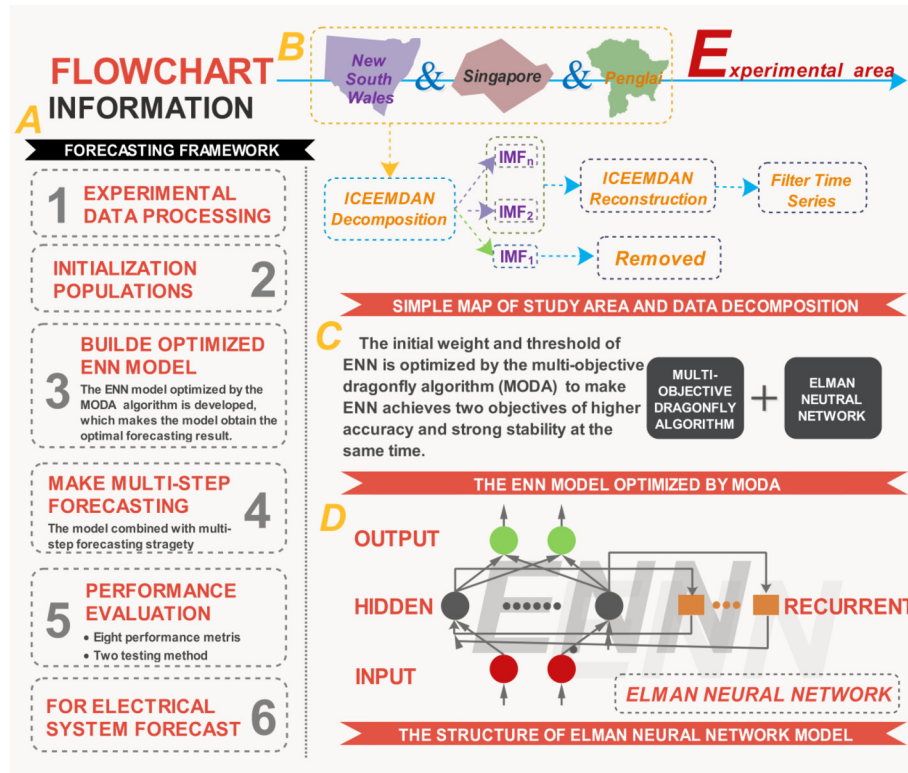


Fig. 1. Flowchart of the developed hybrid forecasting framework.

distribution and consumption in the EPS—named short-term wind speed data, electrical power load data, and electricity price data. The 10 min wind speed data is collected from January 1 to February 7 at two observation sites in Penglai, China, with latitudes from $120^{\circ}43'$ to $120^{\circ}47'$ N and longitudes from $37^{\circ}50'$ to $37^{\circ}37'$ E. The observation site is in a mountainous and hilly area with elevations from 100 to 240 m. The wind turbine generator (WTG) is a type of permanent magnet synchronous generator, with a rated power of 1500 KW, and altitude of measurement of 70 m. The dataset was divided into two sets: the training data set includes 4464 data points (from January 1 to 31), and the testing data set includes 1008 data points (from February 1 to 7). For electrical load time series, two different half-hourly electric load data from New South Wales, Australia are selected as illustrative examples in this paper. The longitudinal data selection [19] is used to divide the raw data into seven subsets to guarantee that the subsets have the same features for improving forecasting performance. For instance, the set of 18 Sundays in March from 2011 to 2014 is denoted as one subset; other subsets are also obtained in the same manner. The last two days of each subset are selected as testing samples, while the rest are treated as training samples. There are seven subsets altogether and two subsets—Wednesday and Sunday—are randomly selected to verify the performance of the developed forecasting framework. For the electricity price time series, two different half-hourly electricity price time series were collected from the New South Wales and Singapore electricity markets from March 1 to 31. The number of training data points is 1248 (from March 1 to 26), and 240 for the testing data points (from 1 March 1 to 26). The descriptive statistical values of six datasets used in this study including the mean, standard deviation, and maximum and minimum numbers are listed in Table 2. The six datasets also listed in table present different characteristics.

4.2. The performance metric

Many performance metrics are employed by researchers for

error evaluation. However, there is no uniform standard for confirming the effectiveness of different models [72]. Thus, in this paper, multiple error criteria are employed to evaluate forecasting performance, including average error (AE), mean absolute error (MAE), root mean square error (RMSE), normalized mean square error (NMSE), mean absolute percentage error (MAPE), index of agreement (IA), fractional bias (FB), and Theil's inequality coefficient (TIC), as listed in Table 3.

4.3. Testing method

Although the metrics mentioned in above section have great significance in evaluating forecasting performance, testing needs to be conducted to confirm effectiveness from a statistical perspective. Thus, two testing methods are used for further comparison, playing indispensable roles in the evaluation module.

4.3.1. Diebold-Mariano test

To verify the significance of the forecasting results of the developed framework outperforming those of the other models, the Diebold-Mariano (DM) test [73] was used to test forecasting accuracy.

The hypothesis tests are:

$$H_0 : E(d_h) = 0, \quad \forall n \quad (11)$$

$$H_1 : E(d_h) \neq 0, \quad \exists n \quad (12)$$

The DM test statistic values equals:

$$DM = \frac{\sum_{h=1}^k \left(L(\epsilon_{t+h}^{(A)}) - L(\epsilon_{t+h}^{(B)}) \right) / k}{\sqrt{S^2/k}} \quad (13)$$

where ϵ_{t+h} denotes the forecast error, S^2 denotes an estimation value for the variance of $d_h = L(\epsilon_{t+h}^{(A)}) - L(\epsilon_{t+h}^{(B)})$, and L denotes the

Table 2
Statistical values of each experiment data.

Mark	Data Set	Mean Value	Standard Deviation	Maximum Value	Minimum Value	Numbers
Short-term wind speed time series						
		(m/s)	(m/s)	(m/s)	(m/s)	(-)
Site 1	All Samples	7.426462	2.947508	17.800000	1.100000	5472
	Training set	7.846102	2.931437	17.800000	1.100000	4464
	Testing set	5.568056	2.208490	13.900000	1.100000	1008
Site 2	All Samples	8.238798	2.982214	18.100000	1.000000	5472
	Training set	8.663172	2.892765	18.100000	1.000000	4464
	Testing set	6.359425	2.626326	16.900000	1.100000	1008
Electrical load time series						
		(MW)	(MW)	(MW)	(MW)	(-)
WED.	All Samples	8461.498529	1181.753378	10724.860000	5890.310000	816
	Training set	8495.950222	1189.386742	10724.860000	5890.310000	720
	Testing set	8203.110833	1094.436921	9478.300000	6046.220000	96
SUN.	All Samples	7323.288264	919.696276	9960.300000	5455.570000	864
	Training set	7343.445482	930.769419	9960.300000	5455.570000	768
	Testing set	7162.030521	812.249181	8401.230000	5710.860000	96
Electricity price time series						
		(\$/MWh)	(\$/MWh)	(\$/MWh)	(\$/MWh)	(-)
NSW.	All Samples	48.677083	3.923924	61.940000	36.270000	1488
	Training set	48.554832	3.996669	61.940000	36.270000	1248
	Testing set	49.312792	3.459983	60.420000	41.490000	240
SG.	All Samples	136.025040	28.989374	563.600000	101.750000	1488
	Training set	137.002853	29.219388	563.600000	101.750000	1248
	Testing set	130.940417	27.259651	355.190000	111.120000	240

(-) indicates without measurement unit.

Table 3

Performance metric rules.

Metric	Definition	Equation
AE	The average error of forecasting results	$\text{AE} = \frac{1}{N} \sum_{i=1}^N (A_i - F_i)$
MAE	The mean absolute error of forecasting results	$\text{MAE} = \frac{1}{N} \sum_{i=1}^N F_i - A_i $
RMSE	The square root of average of the error squares	$\text{RMSE} = \sqrt{\frac{1}{N} \times \sum_{i=1}^N (F_i - A_i)^2}$
NMSE	The normalized average of the squares of the errors	$\text{NMSE} = \frac{1}{N} \sum_{i=1}^N \frac{(F_i - A_i)^2}{F_i A_i}$
MAPE	The average of absolute percentage error	$\text{MAPE} = \frac{1}{N} \sum_{i=1}^N \left \frac{A_i - F_i}{A_i} \right \times 100\%$
IA	The index of agreement of forecasting results	$\text{IA} = 1 - \sum_{i=1}^N (F_i - A_i)^2 / \sum_{i=1}^N (F_i - \bar{A} + A_i - \bar{A})^2$
FB	The fractional bias of forecasting results	$\text{FB} = 2(\bar{A} - \bar{F}) / (\bar{A} + \bar{F})$
TIC	The theil's inequality coefficient of forecasting results	$\text{TIC} = \sqrt{\frac{1}{N} \times \sum_{i=1}^N (F_i - A_i)^2} / \left(\sqrt{\frac{1}{N} \times \sum_{i=1}^N A_i^2} + \sqrt{\frac{1}{N} \times \sum_{i=1}^N F_i^2} \right)$

loss function, which is performed to measure the forecasting accuracy. Two common versions of L are widely used in the studies—absolute deviation error loss and square error loss.

The test statistic DM is convergent to the standard normal distribution. The null hypothesis will be rejected if

$$|DM| > z_{\alpha/2} \quad (14)$$

where $z_{\alpha/2}$ is the critical z-value and α is the significance level.

4.3.2. Forecasting effectiveness

The forecasting effectiveness (FE) can be verified not only via the sum of the squared errors but also through the mean and mean square deviation of the forecasting accuracy. The general description is presented in detail in Ref. [74]:

The k -th-order forecasting effectiveness unit is

$$m^k = \sum_{n=1}^N Q_n A_n^k \quad (15)$$

where Q_n denotes the discrete probability distribution, and $\sum_{n=1}^N Q_n = 1$ (A_n) denotes the forecasting accuracy. If the distribution prior to information is unknown, Q_n is defined as $1/N$.

The k -order forecasting effectiveness is

$$H(m^1, m^2, \dots, m^k) \quad (16)$$

If $H(x) = x$ is a single variable continuous function, the 1st-order FE is the expected forecasting accuracy sequence, which is $H(m^1) = m^1$. Whereas, if $H(x, y) = x(1 - \sqrt{y - x^2})$ is a two-variable continuous function, then the 2nd-order FE describes the difference between the expectation and standard deviation, defined as $H(m^1, m^2) = m^1(1 - \sqrt{m^2 - (m^1)^2})$.

4.4. Experiment setup

To estimate the performance of the developed hybrid forecasting framework for EPS forecasting, three experiments are conducted in this study, including Experiment I: tested with wind speed data, Experiment II: tested with electrical load data, and Experiment III: tested with electricity price data. Four types of comparison researches are conducted in each experiment to successfully and comprehensively verify effectiveness. In this paper, the developed hybrid forecasting framework is denoted as ICEEMDAN-MODA-ENN. In order to verify the superiority of the developed forecasting framework, other forecasting models were

defined as comparison models. Therefore, the single artificial intelligence (AI) models, different decomposition approach-based models, and different optimization algorithm-based models are considered. For single AI models, the generalized regression neural network (GRNN) model and ENN model are implemented as the single benchmark. For different decomposition approach-based models, the original form of the ICEEMDAN, EMD family of the EMD method, and EEMD method, are selected as benchmark models, whereas the single ENN model is used for EPS forecasting (i.e., EMD-ENN, EEMD-ENN). For different optimization algorithm-based models, the particle swarm optimization (PSO) and MODA algorithms are employed to optimize the ENN model (i.e., PSO-ENN, MODA-ENN). In summary, a total of seven compared models are formulated to evaluate the developed hybrid forecasting framework.

4.5. Experiment I: tested with wind speed data

The short-term wind speed data with a 10-min time interval, collected from January 1 to 7 February at two observation sites in Penlai, China, are used to verify the effectiveness of the developed forecasting framework for wind speed forecasting. All the performance metrics for each model are listed in Tables 4 and 5. The values in bold indicate the best values of each criterion among all the models. Moreover, Fig. 2 shows the graphical forecasting results in observation sites 1 and 2, respectively, which all illustrate that the forecasting line of the developed forecasting framework is closer to the observation line than any other compared forecasting lines in all cases. Moreover, the developed forecasting framework achieves the best MAPE among all compared models.

For the short-term wind speed forecasting, Tables 4 and 5, and Fig. 2 respectively list and presents the following:

- (a) In the comparison of single AI models (i.e., GRNN, ENN) in terms of all performance metrics, the ENN model is superior to the GRNN model. For example, at observation site 1, the ENN model achieves the best MAPE at 8.39722%, 10.379568%, and 11.87009% for one-step, two-step, and three-step forecasting, respectively. On the other hand, the GRNN has relatively larger MAPE at 10.139733%, 11.685594%, and 12.908143% for one-step, two-step, and three-step forecasting, respectively. The differences of the results between these two models reveal that the ENN model is powerful for wind speed forecasting, having been employed as the basic forecasting module for the robust hybrid forecasting framework.
- (b) Compared with the single ENN model, all ENN-based models significantly outperformed the ENN model because of the

Table 4

Experimental results of the developed forecasting framework and other models (Experiment I, Observation site 1).

Horizon	Model	AE (m/s)	MAE (m/s)	RMSE (m/s)	NMSE (-)	MAPE (%)	IA (-)	FB (-)	TIC (-)
One-Step	ENN	0.065969	0.408018	0.547745	0.007491	8.397227	0.983715	-0.011778	0.045617
	GRNN	0.053127	0.495965	0.651520	0.010490	10.139733	0.976077	-0.009496	0.054420
	PSO-ENN	0.049308	0.402824	0.539266	0.007136	8.089185	0.984204	-0.008816	0.044972
	EMD-ENN	0.034179	0.254436	0.336100	0.002716	5.107174	0.994025	-0.006120	0.028029
	EEMD-ENN	0.019467	0.206915	0.276912	0.001885	4.246645	0.995938	-0.003490	0.023125
	MODA-ENN	0.047990	0.388837	0.524746	0.006944	7.644727	0.985176	-0.008582	0.043743
	ICEEMDAN-ENN	0.019292	0.178153	0.243061	0.001545	3.628112	0.996873	-0.003459	0.020298
	ICEEMDAN-MODA-ENN	0.012701	0.168536	0.231937	0.001384	3.294953	0.997188	-0.002278	0.019363
Two-Step	ENN	0.082201	0.496528	0.682769	0.011426	10.379568	0.974240	-0.014655	0.056826
	GRNN	0.056382	0.569260	0.756695	0.014374	11.685594	0.967088	-0.010075	0.063237
	PSO-ENN	0.061506	0.487480	0.671238	0.011095	9.875798	0.975062	-0.010986	0.055965
	EMD-ENN	0.057857	0.327612	0.444436	0.004632	6.768409	0.989367	-0.010337	0.037028
	EEMD-ENN	0.034666	0.297854	0.407031	0.003882	6.228679	0.991049	-0.006207	0.033984
	MODA-ENN	0.061825	0.475792	0.657513	0.010715	9.531440	0.976242	-0.011042	0.054798
	ICEEMDAN-ENN	0.039487	0.275276	0.381015	0.003531	5.767277	0.992129	-0.007067	0.031810
	ICEEMDAN-MODA-ENN	0.027555	0.265417	0.365882	0.003171	5.334816	0.992906	-0.004937	0.030530
Three-Step	ENN	0.115433	0.568167	0.754099	0.013818	11.870099	0.968101	-0.020519	0.062644
	GRNN	0.066364	0.624906	0.817327	0.016489	12.908143	0.960990	-0.011848	0.068299
	PSO-ENN	0.080509	0.547324	0.727809	0.013027	11.125128	0.970269	-0.015160	0.060611
	EMD-ENN	0.083214	0.393970	0.547725	0.007168	8.242357	0.983547	-0.014834	0.045586
	EEMD-ENN	0.058871	0.384462	0.543543	0.006754	8.238854	0.983652	-0.010517	0.045348
	MODA-ENN	0.095415	0.538539	0.722659	0.013013	10.886456	0.970762	-0.016991	0.060127
	ICEEMDAN-ENN	0.071158	0.369042	0.524325	0.006342	7.915580	0.984716	-0.012699	0.043719
	ICEEMDAN-MODA-ENN	0.047563	0.353436	0.504984	0.005775	7.286489	0.986277	-0.008506	0.042099

(-) indicates without measurement unit; The values in bold indicate the best values of error metrics.

Table 5

Experimental results of the developed forecasting framework and other models (Experiment I, Observation site 2).

Horizon	Model	AE (m/s)	MAE (m/s)	RMSE (m/s)	NMSE (-)	MAPE (%)	IA (-)	FB (-)	TIC (-)
One-Step	ENN	0.061868	0.421089	0.580555	0.006377	7.433177	0.987122	-0.009681	0.042137
	GRNN	0.049428	0.507880	0.694862	0.009115	8.931500	0.981155	-0.007742	0.050531
	PSO-ENN	0.046303	0.423746	0.589358	0.006344	7.215407	0.986947	-0.007255	0.042770
	EMD-ENN	0.010686	0.235745	0.313706	0.001727	4.106712	0.996340	-0.001679	0.022818
	EEMD-ENN	0.034376	0.220065	0.298455	0.001642	3.847846	0.996712	-0.005391	0.021663
	MODA-ENN	0.045948	0.405807	0.571757	0.006401	6.887751	0.987662	-0.007199	0.041508
	ICEEMDAN-ENN	0.020270	0.184002	0.245929	0.000995	3.293740	0.997757	-0.003182	0.017874
	ICEEMDAN-MODA-ENN	0.009755	0.168931	0.236018	0.000977	2.929178	0.997957	-0.001533	0.017153
Two-Step	ENN	0.085127	0.526515	0.735519	0.010318	9.325575	0.979018	-0.013297	0.053331
	GRNN	0.053263	0.584977	0.801245	0.012174	10.306113	0.974586	-0.008341	0.058288
	PSO-ENN	0.068194	0.523728	0.737104	0.010255	8.842341	0.979337	-0.010666	0.053436
	EMD-ENN	0.025527	0.328713	0.467506	0.004052	5.758049	0.991717	-0.004006	0.034005
	EEMD-ENN	0.065654	0.323248	0.458334	0.003919	5.687590	0.992165	-0.010271	0.033212
	MODA-ENN	0.067292	0.506177	0.725055	0.010177	8.604056	0.979918	-0.010526	0.052583
	ICEEMDAN-ENN	0.040093	0.290513	0.403488	0.002695	5.228552	0.993841	-0.006285	0.029320
	ICEEMDAN-MODA-ENN	0.021234	0.265825	0.393129	0.002807	4.583959	0.994276	-0.003333	0.028561
Three-Step	ENN	0.115412	0.585206	0.806129	0.012290	10.475743	0.974392	-0.017985	0.058381
	GRNN	0.065234	0.641470	0.873402	0.014644	11.249197	0.969477	-0.010206	0.063514
	PSO-ENN	0.104371	0.572134	0.792548	0.011810	9.806887	0.975656	-0.016279	0.057379
	EMD-ENN	0.053750	0.429688	0.647409	0.007798	7.565680	0.983805	-0.008416	0.047042
	EEMD-ENN	0.105649	0.443371	0.649052	0.007954	7.798450	0.984117	-0.016476	0.046921
	MODA-ENN	0.093008	0.559002	0.785416	0.011949	9.562243	0.976072	-0.014519	0.056911
	ICEEMDAN-ENN	0.064700	0.401820	0.591108	0.006186	7.201649	0.986506	-0.010122	0.042926
	ICEEMDAN-MODA-ENN	0.037799	0.376373	0.581587	0.006654	6.366034	0.987364	-0.005926	0.042215

(-) indicates without measurement unit; The values in bold indicate the best values of error metrics.

contribution of the decomposition approach and optimization algorithms. Besides, the contribution of data pre-processing to the final improvements is more than those of the optimization algorithms. For example, for one-step forecasting at observation site 1, the ICEEMDAN approach leads to reductions of 0.046678 in AE, 0.229865 in MAE, 0.304684 in RMSE, 0.005946 in NMSE, 4.769116% in MAPE, 0.013158 in IA, 0.008319 in FB, and 0.025319 in TIC, whereas the MODA algorithm contributes to performance improvements of 0.017979 in AE, 0.019182 in MAE, 0.022999 in RMSE, 0.000547 in NMSE, 0.752501% in MAPE, 0.001461 in IA, 0.003196 in FB, and 0.001874 in TIC.

(c) In the comparison between the models based on different decomposition approaches or optimizers, it is obvious that the ICEEMDAN approach (i.e., ICEEMDAN-ENN) is superior to models with EMD and EEMD methods (i.e., EMD-ENN and EEMD-ENN) in all cases, and the MODA algorithm (MODA-ENN) performs much better than the models optimized by the well-known single-objective optimization PSO algorithms (i.e., PSO-ENN). Accordingly, it can be reasonably concluded that the ICEEMDAN approach is superior to the EMD and EEMD decomposition approaches for data pre-processing, whereas the MODA algorithms outperform the single-objective optimization algorithm in optimizing the

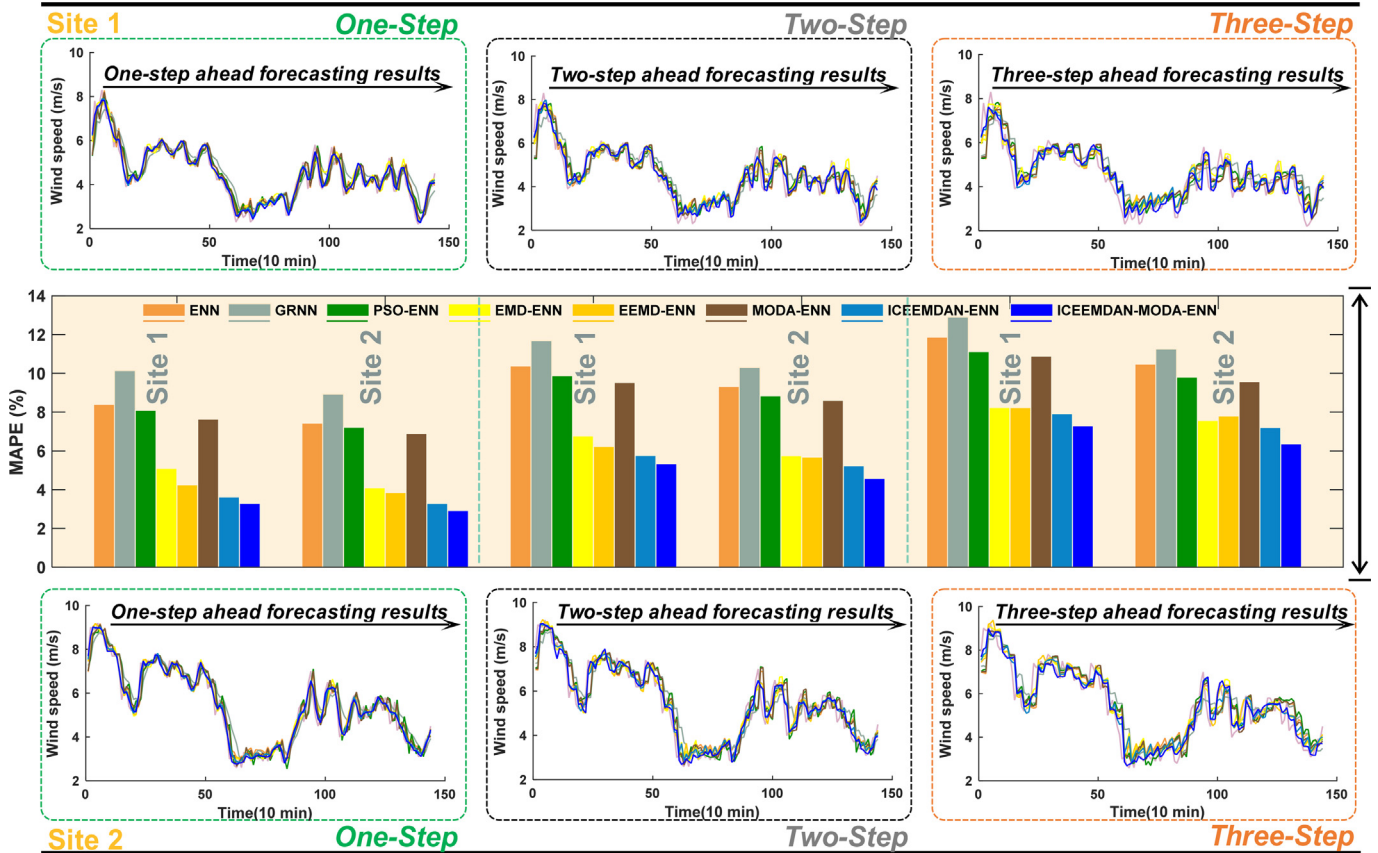


Fig. 2. The forecasting result in two observation sites.

parameters of the model by taking into consideration the simultaneous realization of the objectives of high accuracy and stability.

- (d) Statistics in observation site 1 show that the MAPE values of the developed hybrid forecasting framework are 3.294953%, 5.334816%, and 7.286489% for one-step, two-step, and three-step forecasting, respectively, whereas the MAPE values offered by observation site 2 are 2.929178%, 4.583959%, and 6.366034%, for one-step, two-step, and three-step forecasting, respectively. The experiments conducted on these two sites prove that the developed forecasting framework can effectively forecast future variations in wind speed. More detailed comparison results among all models are listed in Tables 4 and 5.

Remarks. Based on the above analyses, including the comparison of all performance metrics, the developed forecasting framework performs better in almost all of the cases. The combination of the beneficial components capitalizes on the strength of each part, resulting to the better performance of the developed forecasting framework than the other models in terms of accuracy and stability. Therefore, the forecasting framework can be employed as an effective wind speed forecasting approach for the EPS.

4.6. Experiment II: tested with electrical load data

Experiment II is aimed at verifying the performance of the developed hybrid forecasting framework in terms of electrical load

forecasting in the EPS. Tables 6 and 7 list the forecasting results given by the developed forecasting framework and other models. The first day results in each testing sample are depicted in Figs. 3 and 4, which reveal that the developed forecasting framework is superior to the benchmark models in terms of electrical load forecasting. The results of the electrical power load forecasting presented in the aforementioned tables and figures clearly showed the following:

- (a) For the electrical load data of Wednesday and all forecasting steps, the developed hybrid forecasting framework achieves the best forecasting performance in three-step forecasting with a MAPE of 0.982396%. Moreover, except for the GRNN model, the single ENN model has the worst performance. The MAPE of this model increases by 0.562832% compared with that of the developed forecasting framework because the ICEEMDAN removes noise in the raw time series and guarantees that the main feature can be successfully and effectively extracted and identified. Meanwhile, the MODA algorithm optimizes the ENN model and makes the model simultaneously achieve high accuracy and stability. It is found that the developed forecasting framework is more effective in electrical load forecasting. Furthermore, it is fully demonstrated that above components can effectively boost forecasting performance and be combined with other methods so that it can be widely employed in other fields.
- (b) When comparing the developed hybrid forecasting framework with the ENN based model, ICEEMDAN-ENN, and MODA-ENN, the function of each component can be presented clearly. For example, on Wednesday, the ICEEMDAN

Table 6
Experimental results of the developed forecasting framework and other models (Experiment II, Wednesday).

Metric	GRNN	ENN			PSO-ENN			MODA-ENN		
		1-Step		2-Step	3-Step	1-Step	2-Step	3-Step	1-Step	2-Step
		1-Step	2-Step	3-Step	1-Step	2-Step	3-Step	1-Step	2-Step	3-Step
AE (MW)										
AE (MW)	19.149781	26.314379	33.410773	8.627282	11.3523902	14.555489	11.931391	18.852392	27.284954	8.866554
MAE (MW)	87.948129	108.650371	132.537690	74.941738	106.423450	122.214431	69.648784	103.6328794	121.038799	68.236294
RMSE (MW)	107.326485	141.123404	178.297756	93.991675	135.389609	158.462118	88.450097	130.470154	160.045588	86.990100
NMSE (-)	0.00156	0.000425	0.000271	0.000114	0.000239	0.000324	0.000103	0.000225	0.000223	0.000101
MAPE (%)	1.108750	1.370734	1.689530	0.950533	1.345842	1.545228	0.874583	1.304168	1.531070	0.852753
IA (-)	0.997527	0.995719	0.993084	0.998103	0.996033	0.994452	0.998326	0.996350	0.994388	0.998383
FB(-)	-0.002332	-0.003203	-0.004065	-0.001051	-0.001383	-0.001773	-0.001453	-0.002296	-0.003321	-0.001080
TIC(-)	0.006478	0.008515	0.010754	0.005677	0.008177	0.009570	0.005341	0.00785	0.009657	0.005254
EMD-ENN										
Metric	EMD-ENN	ENN			ICEMD-ENN			ICEMD-MODA-ENN		
		1-Step		2-Step	3-Step	1-Step	2-Step	3-Step	1-Step	2-Step
		1-Step	2-Step	3-Step	1-Step	2-Step	3-Step	1-Step	2-Step	3-Step
AE (MW)	6.841415	16.303463	27.915681	8.610090	15.227078	23.454959	3.2165582	5.797947	9.455179	5.880449
MAE (MW)	41.401170	63.542622	97.927472	36.287600	60.930793	85.577657	35.913861	60.330441	81.470704	30.612325
RMSE (MW)	52.807974	88.130735	132.594677	46.690418	80.185583	122.277727	45.188301	80.569141	112.986086	38.041931
NMSE (-)	0.000039	0.000108	0.000236	0.000085	0.000228	0.000195	0.000028	0.000091	0.000171	0.000019
MAPE (%)	0.511294	0.796424	1.239528	0.459621	0.768968	1.081113	0.445678	0.746576	1.020346	0.386894
IA (-)	0.999408	0.998341	0.996207	0.999536	0.998624	0.996771	0.999565	0.998608	0.997236	0.999692
FB(-)	-0.000834	-0.001986	-0.003397	-0.001049	-0.001855	-0.002855	-0.000392	-0.000707	-0.001152	-0.000717
TIC(-)	0.003190	0.005320	0.008000	0.002820	0.004841	0.007379	0.002730	0.004867	0.006824	0.002298

(-) indicates without measurement unit.

approach increases the MAPE by 0.465865%, 0.532114%, and 0.492339% for one-step, two-step and three-step forecasting, respectively. On the other hand, the MODA method improves the MAPE by 0.058789, 0.070103%, and 0.037951%, respectively. However, it is necessary to point out that although the MODA improved absolute MAPE by small values, it effected significant improvement in terms of the decreased relative error (RE) of MAPE.

- (c) In order to further analyze the influence of different decomposition approaches and optimizers, corresponding comparison studies are conducted in this experiment. All the comparison results for the electrical load of Wednesday and Sunday reveal that these two approaches used in this paper are superior to other compared approaches. This explains why these two methods are successfully and effectively employed in this research.
- (d) The electrical load data of Wednesday and Sunday have different characteristics according to the statistical values listed in Table 2. These two days can be represented as workday and non-workday, respectively. For example, the MAPE values of the developed forecasting framework for Wednesday are 0.386889%, 0.676894%, and 0.982396% in one-step, two-step, and three-step forecasting, respectively. On the other hand, the MAPE values of Sunday are 0.374590%, 0.619835%, and 0.852979% in one-step, two-step, and three-step forecasting, respectively. From the lists of Tables 6 and 7, it can be concluded that the developed forecasting framework performs better in all cases.

Remarks. The developed hybrid forecasting framework has better accuracy than other models in terms of electric power load forecasting. Based on the two experiments above, the developed hybrid forecasting framework is determined to be the best among all other models. Moreover, because of the applicability the framework in these two signals, which feature different characteristics, it can reasonably be concluded that the developed forecasting framework has universal applicability. Evidently, the developed framework is effective for electrical power load and wind speed forecasting.

4.7. Experiment III: tested with electricity price data

In this study, two electricity price data collected from the electricity markets of Australia and Singapore are applied to the empirical study to estimate the performance of the proposed novel forecasting framework for electricity price forecasting in the EPS. In the Australian market, the half-hour electricity price series of New South Wales (NSW) are adopted, while in the Singaporean market, the half-hourly data of Singapore (SG) are selected. The main reason for selecting New South Wales and Singapore as study areas is their significant difference in terms of geographical positions, climatic characteristics, economic development, regional scales, and industrial structures. If the developed hybrid forecasting framework performs better in significantly different environments, it could be reasonably concluded that the developed forecasting framework has remarkable effectiveness and wide applicability for electricity price forecasting. More importantly, if it is found from the two experiments that the developed hybrid forecasting framework is applicable and suitable, it can be concluded that not only does it have wide applicability but it is also effective and practicable in EPS forecasting.

The overall performances of the forecasting models, as well as the forecasting results and specific error evaluation metric values are listed in Tables 8 and 9 and shown Fig. 5, from which it can be

Table 7

Experimental results of the developed forecasting framework and other models (Experiment II, Sunday).

Metric	GRNN			ENN			PSO-ENN				MODA-ENN	
	1-Step	2-Step	3-Step	1-Step	2-Step	3-Step	1-Step	2-Step	3-Step	1-Step	2-Step	3-Step
AE (MW)	7.750992	12.306712	12.579726	6.495592	3.534221	-8.300117	3.914621	-1.161949	-11.828018	7.989659	6.100477	-0.919065
MAE (MW)	93.040044	123.023027	141.810137	63.056560	84.852107	99.301374	62.881412	83.601278	97.069484	62.224985	82.007702	95.330988
RMSE (MW)	115.717150	154.405532	189.135481	86.253197	117.839456	129.576628	86.968334	119.039766	126.311141	86.011398	116.370398	125.762297
NMSE (-)	0.000249	0.000442	0.000692	0.000132	0.000258	0.000330	0.000134	0.000262	0.000317	0.000132	0.000254	0.000311
MAPE (%)	1.314884	1.746839	1.997903	0.892986	1.188879	1.382024	0.889475	1.166943	1.335137	0.880073	1.147519	1.322171
IA (-)	0.994668	0.990405	0.985630	0.997118	0.994605	0.993268	0.997066	0.994472	0.993590	0.997138	0.994745	0.993712
FB(-)	-0.001082	-0.001717	-0.001755	-0.000907	-0.000493	0.001160	-0.000546	0.000162	0.001653	-0.001115	-0.000851	0.000128
TIC(-)	0.008025	0.010705	0.013112	0.005981	0.008173	0.008996	0.006032	0.008259	0.008772	0.005964	0.008070	0.008727
Metric	EMD-ENN			EEMD-ENN			ICEEMD-ENN				ICEEMD-MODA-ENN	
	1-Step	2-Step	3-Step	1-Step	2-Step	3-Step	1-Step	2-Step	3-Step	1-Step	2-Step	3-Step
AE (MW)	2.504434	5.445387	10.658824	5.600636	9.105311	14.185349	5.720724	10.119869	13.975400	2.179991	3.549774	4.659143
MAE (MW)	39.344162	58.376572	80.955963	38.334072	57.890721	77.419706	31.145771	49.814363	67.989475	26.298636	43.878961	61.493413
RMSE (MW)	51.714931	74.791461	111.874960	53.310709	78.988680	106.637101	45.629892	73.002494	95.623023	38.139578	61.883103	97.267453
NMSE (-)	0.000044	0.000102	0.000242	0.000051	0.000114	0.000219	0.000035	0.000094	0.000175	0.000025	0.000071	0.000181
MAPE (%)	0.573057	0.835979	1.140278	0.547446	0.824537	1.078376	0.447612	0.709133	0.951331	0.374590	0.619835	0.852979
IA (-)	0.998970	0.997833	0.995096	0.998904	0.997582	0.995555	0.999199	0.997941	0.996444	0.999440	0.998517	0.996295
FB(-)	-0.000350	-0.000760	-0.001487	-0.000782	-0.001271	-0.001979	-0.000798	-0.001412	-0.001949	-0.000304	-0.000496	-0.000650
TIC(-)	0.003587	0.005187	0.007756	0.003697	0.005477	0.007391	0.003164	0.005061	0.006628	0.002646	0.004292	0.006746

(-) indicates without measurement unit.

observed that the superiority of the hybrid forecasting framework developed in this paper is evident. The detailed comparisons are as follows.

- (a) For the electricity price time series of NSW and SG, the developed hybrid forecasting framework performs better in almost all of the performance metrics, as can be seen from the bold values listed in [Tables 8 and 9](#). Except for the AE and FB metrics, the values in the column of the developed forecasting framework is presented in bold indicating these as the best values under each metric among all models. Based on the experiments using the NSW and SG data, it can be concluded that the developed framework can effectively forecast future electricity prices.
- (b) The comparisons also account for the same conclusions reached in Experiment I and Experiment II, i.e., the developed forecasting framework is superior to all considered benchmark models and can be effectively used for EPS forecasting. The results once again prove the forecasting effectiveness of the hybrid forecasting framework and its components, especially so as electricity price has the most irregular data in the three signals studied.
- (c) In NSW, MAPE values obtained by using the developed forecasting framework is 0.886567%, 1.339390%, and 2.022866% for one-step, two-step, and three-step forecasting, respectively. In SG, the MAPE values are 2.068847%, 3.039620%, and 4.042885% for one-step, two-step, and three-step forecasting, respectively. It is important to note that forecasting accuracy vary in different areas, mainly because of the difference in environments as mentioned above. In other words, differences in forecasting accuracies are inevitable and objective. What are of primary importance in its use are the forecasting effectiveness and applicability offered by the developed forecasting framework.
- (d) Through the above three experiments for different signals in EPS and based on all comparison results, the developed hybrid forecasting framework is applicable and suitable. It can therefore be concluded as effective and suitable for EPS forecasting.

Remarks. Based on the analysis of the experimental results, it is believed that the hybrid forecasting framework performs better than the benchmark models for forecasting future changes in electricity prices. Moreover, the developed hybrid forecasting framework not only has wide applicability for the same indicator in different environments but also effective and practicable in EPS forecasting.

5. Discussion

Insights on the comparative studies, is conducted in this section, which includes the significance of forecasting results, effectiveness of each component, forecasting steps and computational time.

5.1. Discussion of the significance of forecasting results

To test the significance of the outperformance of the developed forecasting framework over the other models, the DM test is used. The test is used to determine the case that will allow rejection of the null hypothesis at a given significance level. The DM statistical values calculated by the square error loss function are listed in [Table 10](#), which indicates that (a) the DM test values of the GRNN, ENN, PSO-ENN, and MODA-ENN models are greater than the critical value of the 1% significance level, and the DM test values of the EMD-ENN and EEMD-ENN models are greater than the critical value of the 5% significance level; (b) the developed forecasting framework significantly outperforms the other compared models at different significance levels. Thus, it can reasonably be concluded that the developed hybrid forecasting framework is superior to the comparison models.

The FE was employed to measure the degree of forecasting accuracy as listed in [Table 10](#), in which the values in bold indicate the best values among all the models. The results show that (a) the 1st-order forecasting effectiveness offered by the developed forecasting framework is greater than at least 0.93, whereas the 2nd-order values are greater than 0.85; (b) the FE values of the developed forecasting framework are greater than those of the other considered models in all experiments, whether for 1st-order or 2nd-order forecasting effectiveness. Therefore, the developed framework is significantly superior to all compared models.

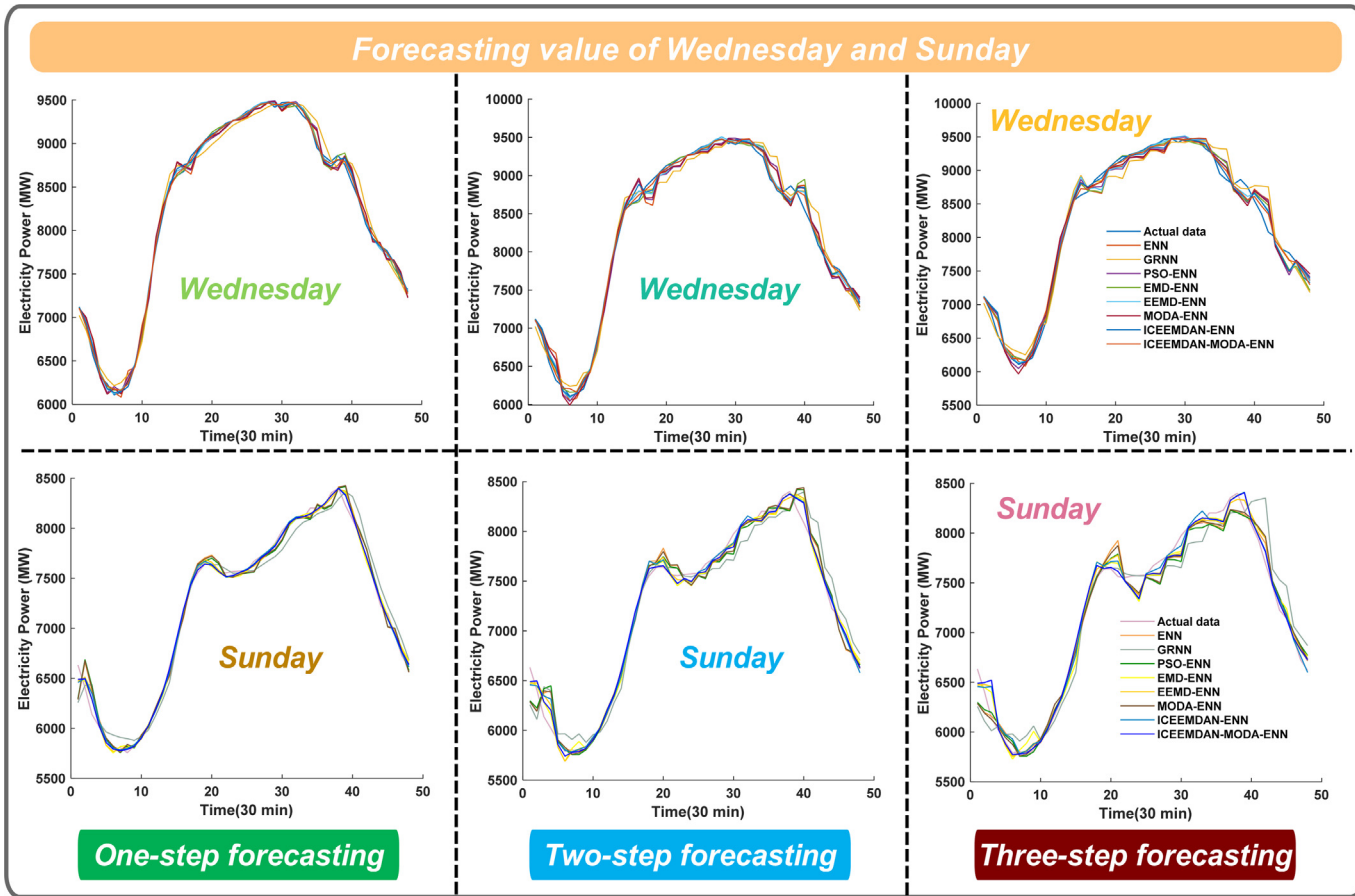


Fig. 3. The forecasting results of Wednesday and Sunday.

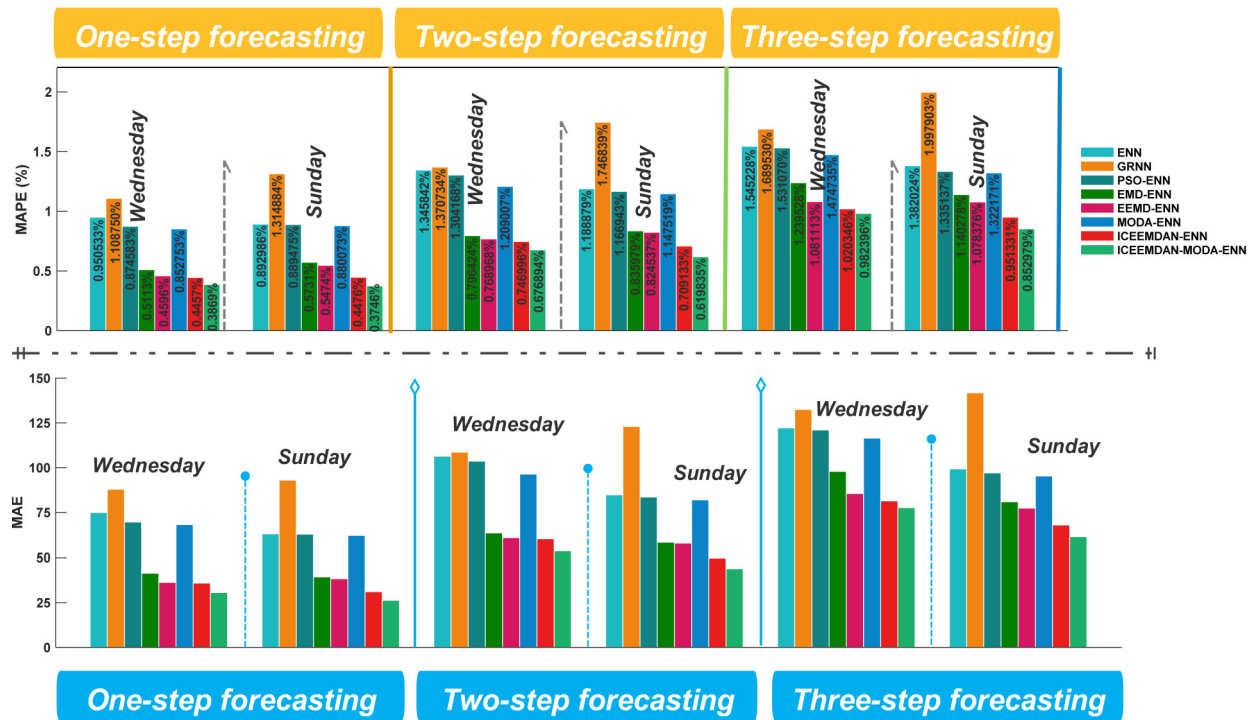


Fig. 4. The MAPE and MAE of Wednesday and Sunday.

Table 8

Experimental results of the developed forecasting framework and other models (Experiment III, New South Wales).

Horizon	Metric	GRNN	ENN	EMD-ENN	EEMD-ENN	ICEEMDAN-ENN	PSO-ENN	MODA-ENN	ICEEMDAN-MODA-ENN
One-Step	AE (\$/MWh)	−0.190696	−0.053415	−0.070639	0.002207	−0.027015	−0.033000	−0.096618	−0.08098
	MAE (\$/MWh)	1.224768	1.088784	0.736141	0.523796	0.452194	1.081832	1.051323	0.440724
	RMSE (\$/MWh)	1.745356	1.531314	0.982157	0.749954	0.621659	1.482736	1.467492	0.626155
	NMSE (−)	0.001272	0.000981	0.000403	0.000242	0.000162	0.000909	0.000903	0.000167
	MAPE (%)	2.466007	2.193610	1.484002	1.052588	0.912424	2.186419	2.113999	0.886567
	IA (−)	0.927499	0.946020	0.979439	0.987830	0.991716	0.948661	0.950011	0.991543
	FB(−)	0.003875	0.001084	0.001433	−0.000045	0.000548	0.000669	0.001961	0.000164
	TIC(−)	0.017690	0.015499	0.009941	0.007586	0.006290	0.015005	0.014860	0.006334
Two-Step	AE (\$/MWh)	−0.224920	−0.112170	−0.155216	−0.019240	−0.089868	−0.079067	−0.182779	−0.045931
	MAE (\$/MWh)	1.355923	1.315213	0.985627	0.734728	0.675695	1.309102	1.268272	0.663805
	RMSE (\$/MWh)	1.913196	1.834211	1.336540	1.027493	0.972309	1.803093	1.781547	0.917915
	NMSE (−)	0.001507	0.001374	0.000744	0.000455	0.000394	0.001330	0.001305	0.000355
	MAPE (%)	2.741697	2.669318	1.985937	1.475248	1.366934	2.659263	2.571318	1.339390
	IA (−)	0.911283	0.918981	0.961227	0.976856	0.979662	0.920168	0.923169	0.981657
	FB(−)	0.004572	0.002277	0.003153	0.000390	0.001824	0.001605	0.003713	0.000932
	TIC(−)	0.019399	0.018577	0.013540	0.010395	0.009844	0.018256	0.018056	0.009289
Three-Step	AE (\$/MWh)	−0.159227	−0.153213	−0.026693	−0.070863	−0.110571	−0.090056	−0.187094	−0.047545
	MAE (\$/MWh)	1.517627	1.386824	1.156928	1.104121	1.014109	1.404825	1.303901	0.992839
	RMSE (\$/MWh)	2.170250	2.027614	1.688743	1.600335	1.574688	1.971845	1.892524	1.513824
	NMSE (−)	0.001935	0.001684	0.001146	0.001039	0.000992	0.001587	0.001475	0.000922
	MAPE (%)	3.069172	2.814573	2.360776	2.248309	2.066520	2.862695	2.640348	2.022866
	IA (−)	0.880904	0.901025	0.935218	0.943469	0.945739	0.904878	0.912428	0.948971
	FB(−)	0.003234	0.003112	0.000541	0.001438	0.002245	0.001828	0.003801	0.000965
	TIC(−)	0.021991	0.020543	0.017087	0.016199	0.015945	0.019967	0.019182	0.015320

(−) indicates without measurement unit; The values in bold indicate the best values of error metrics.

Table 9

Experimental results of the developed forecasting framework and other models (Experiment III, Singapore).

Horizon	Metric	GRNN	ENN	EMD-ENN	EEMD-ENN	ICEEMDAN-ENN	PSO-ENN	MODA-ENN	ICEEMDAN-MODA-ENN
One-Step	AE (\$/MWh)	2.288229	1.024573	0.440381	0.726016	1.145345	1.306489	1.336329	0.897700
	MAE (\$/MWh)	10.461679	6.634191	4.803712	3.788451	3.580998	6.473009	6.363004	3.352902
	RMSE (\$/MWh)	24.774001	15.286942	10.489647	9.585151	9.328685	15.098151	15.382853	8.984401
	NMSE	0.127152	0.032722	0.012570	0.011882	0.011522	0.029948	0.030256	0.010970
	MAPE (%)	6.977212	4.253822	3.187077	2.397353	2.260561	4.188059	4.123818	2.068847
	IA	0.759091	0.904688	0.961814	0.969114	0.971162	0.909360	0.911191	0.972589
	FB	−0.017324	−0.007794	−0.003358	−0.005529	−0.008709	−0.009928	−0.010154	−0.006832
	TIC	0.091748	0.057059	0.039151	0.035716	0.034698	0.056276	0.057270	0.034466
Two-Step	AE (\$/MWh)	2.423201	2.425058	0.743340	0.988759	1.808615	2.179715	2.218946	1.328409
	MAE (\$/MWh)	11.323199	8.469886	6.747520	5.508925	5.378639	7.934982	7.741764	4.737331
	RMSE (\$/MWh)	25.581699	18.860530	15.135679	12.534933	12.198700	18.194860	17.774613	10.866944
	NMSE	0.130186	0.044674	0.026239	0.020153	0.019164	0.039747	0.036496	0.015749
	MAPE (%)	7.581212	5.562988	4.458907	3.573023	3.506863	5.278774	5.176657	3.039620
	IA	0.739480	0.861471	0.917982	0.946706	0.950802	0.870289	0.884349	0.958681
	FB	−0.018336	−0.018350	−0.005661	−0.007523	−0.013718	−0.016509	−0.016804	−0.010094
	TIC	0.094697	0.069937	0.056424	0.046653	0.045246	0.067549	0.065908	0.040430
Three-Step	AE (\$/MWh)	0.635553	0.624267	0.607697	0.776031	2.272639	0.953495	0.894397	1.453311
	MAE (\$/MWh)	10.989290	8.384616	8.418395	7.036493	6.498691	8.020110	7.784998	5.952191
	RMSE (\$/MWh)	19.605208	16.297322	17.103631	13.211545	13.031966	16.631795	16.204368	11.755410
	NMSE	0.047471	0.034622	0.027251	0.018804	0.020486	0.033859	0.029300	0.015741
	MAPE (%)	7.563379	5.705776	5.786282	4.853347	4.446116	5.440865	5.314314	4.042885
	IA	0.743314	0.858046	0.875864	0.936930	0.940767	0.865434	0.884986	0.948031
	FB	−0.004842	−0.004756	−0.004630	−0.005909	−0.017207	−0.007255	−0.006807	−0.011038
	TIC	0.073701	0.061158	0.063976	0.049270	0.048304	0.062254	0.060578	0.043774

(−) indicates without measurement unit; The values in bold indicate the best values of error metrics.

5.2. Discussion on the effectiveness of each component

In this section, the effectiveness of the data preprocessing approach and optimization algorithm are discussed in detail. To do this, a new evaluation criterion called decreased relative error (RE) of MAPE is employed, which reveals the contributions of each component for the final completion of the developed forecasting framework. This criterion is defined as

$$RE_{MAPE_{ij}} = \frac{MAPE_{model_i} - MAPE_{model_j}}{MAPE_{model_i}} \times 100\% \quad (17)$$

Take Experiment I as an example. By contrasting the results of

the MODA-ENN model and the developed forecasting framework (or contrasting the results of the ENN model and the ICEEMDAN-ENN model), the effectiveness of the decomposition approach can be evaluated by a quantitative value: it improves the MAPE values by 57.185829%, 45.376276%, and 33.246805% for the one-step, two-step, and three-step forecasting, respectively, which reveal that the approach can significantly improve forecasting performance. Besides, by comparing the RE values between the ICEEMDAN-ENN model and either the EMD-ENN or EEMD-ENN models, the contribution of ICEEMDAN can be quantified along with other data decomposition methods. The values listed in Table 11 indicate that the ICEEMDAN approach is superior to all other approaches.

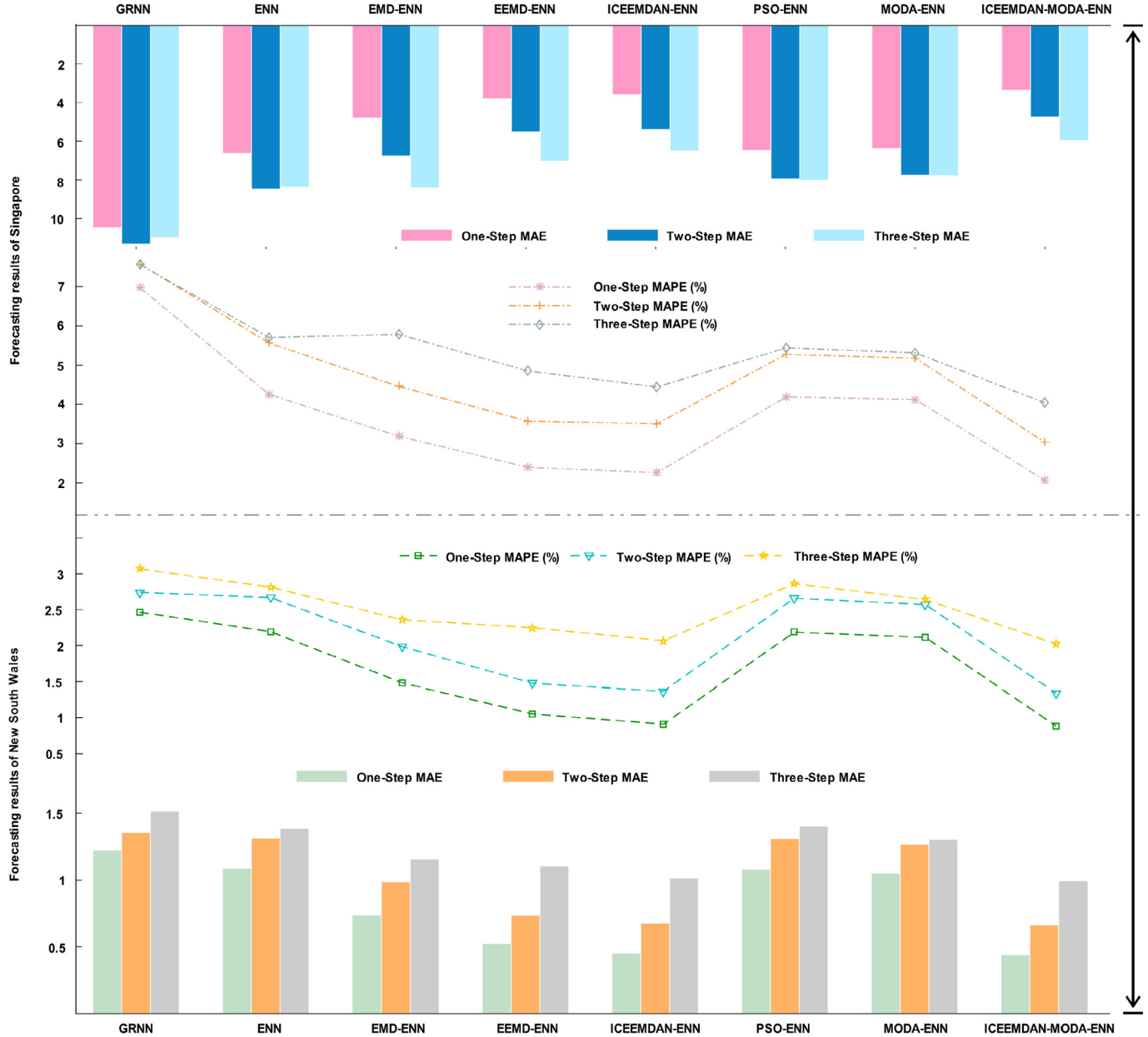


Fig. 5. The results of comparisons between different models.

However, although the multi-objective optimization algorithm in this study was successfully applied, its effectiveness need to be evaluated. It can be defined as the RE values of the ICEEMDAN-ENN model and the forecasting framework (or the ENN model and the MODA-ENN model). The RE values are 10.125519%, 9.913425%, and 9.775300% for the one-step, two-step, and three-step forecasting, respectively, which prove that the optimization method also contributes greatly to the overall success of the framework. Meanwhile, to verify the superiority of multi-objective optimization over a single-objective optimization, a comparison of the MODA-ENN model and PSO-ENN model is conducted. As listed in Table 11, the multi-objective optimization algorithm improves the MAPE values to 5.017772%, 3.090853%, and 2.319983% for the one-step, two-step, and three-step forecasting, respectively proving that the forecasting framework-based MODA yields more accurate and stable forecasting than the framework based single-objective optimization algorithm.

5.3. Discussion of the steps of forecasting

To verify the forecasting effectiveness of the developed framework for EPS, the steps of forecasting are discussed in this section. The comparison results are listed in Table 12. The difference between one-step and two-step wind speed forecasting is 1.847322%, whereas between one-step and three-step, the difference is 3.714196%, which are the worst conditions from the perspective of magnitude. On the other hand, the corresponding differences between the same steps above and electrical load forecasting are 0.267625% and 0.536948%, which are the best conditions also from the perspective of magnitude. Besides, for electricity price forecasting, the one-step forecasting accuracy increases by 0.711798% and 1.555168%, over the second-step and third-step, respectively. These forecasting differences are within an acceptable scale. Accordingly, the developed forecasting framework can be an effective tool for multi-step forecasting in the EPS.

Table 10

Results for the DM test and the FE.

Testing method	Average Value	Experiment I			Experiment II			Experiment III		
		1-Step	2-Step	3-Step	1-Step	2-Step	3-Step	1-Step	2-Step	3-Step
DM-test	ENN	13.245667*	11.560882*	11.150187*	5.672098*	5.218147*	3.278094*	5.183969*	4.867647*	3.026730*
	GRNN	14.305262*	12.375441*	12.202701*	6.472226*	5.595546*	3.679413*	4.668203*	4.237636*	3.386472*
	PSO-ENN	12.870738*	10.859301*	10.506669*	5.503275*	5.180864*	3.278517*	5.230326*	4.827882*	3.136407*
	EMD-ENN	10.355302*	6.013729*	3.276791*	4.393206*	2.877276*	2.901000*	4.408295*	4.275052*	2.342160**
	EEMD-ENN	10.696083*	6.887656*	4.982344*	4.170216*	3.807812*	2.162106**	2.825370*	2.468755*	1.968743**
	MODA-ENN	12.669849*	10.599706*	10.193369*	5.461765*	4.929654*	2.818587*	5.425786*	4.800188*	2.869207*
	ICEEMDAN-ENN	2.981160*	1.787800***	1.767166***	3.384655*	2.588705*	1.968077**	2.433344**	1.988989**	1.764695***
Forecasting effectiveness ^a	ENN	0.92111	0.901934	0.888837	0.990782	0.987326	0.985364	0.967763	0.958838	0.957398
	GRNN	0.905069	0.890467	0.879806	0.987882	0.984412	0.981563	0.953015	0.948617	0.946837
	PSO-ENN	0.923477	0.906422	0.895461	0.991180	0.987644	0.985669	0.968128	0.960310	0.958482
	EMD-ENN	0.953931	0.937368	0.921003	0.994578	0.991838	0.988101	0.976645	0.967776	0.959265
	EEMD-ENN	0.959528	0.940419	0.920088	0.994965	0.992032	0.989203	0.982750	0.974759	0.964492
	MODA-ENN	0.927338	0.909323	0.897757	0.991336	0.988217	0.986015	0.968811	0.961260	0.960227
	ICEEMDAN-ENN	0.965391	0.945021	0.924635	0.995534	0.992719	0.990142	0.984135	0.975631	0.967437
Forecasting effectiveness ^b	ENN	0.968879	0.950406	0.931818	0.996405	0.993972	0.991133	0.985223	0.978105	0.969671
	GRNN	0.84079	0.804189	0.781075	0.982674	0.975874	0.973114	0.927361	0.906717	0.911719
	PSO-ENN	0.819487	0.793361	0.775355	0.979037	0.972039	0.965425	0.900314	0.893238	0.899095
	EMD-ENN	0.851994	0.820887	0.801669	0.983171	0.976269	0.973189	0.925417	0.905519	0.906809
	EEMD-ENN	0.910331	0.872157	0.834593	0.989880	0.984655	0.977122	0.946000	0.923764	0.904748
	MODA-ENN	0.858360	0.824169	0.803102	0.983495	0.977322	0.973898	0.923642	0.905487	0.906675
	ICEEMDAN-ENN	0.928823	0.882509	0.837426	0.991256	0.985395	0.980367	0.959836	0.942957	0.926462
	ICEEMDAN-MODA-ENN	0.937937	0.898084	0.857075	0.993048	0.98046	0.980902	0.961465	0.948803	0.930895

The values in bold indicate the best values of error metrics.

* Indicates the 1% significance level, ** indicates the 5% significance level, *** indicates the 10% significance level.

- ^a Indicates the 1st-order forecasting effectiveness.
^b Indicates the 2nd-order forecasting effectiveness.

5.4. Computational time

Table 13 lists the average values of the computational times for the three experiments carried out in MATLAB R2015a in Windows 7 with 3.30 GHz Intel Core i5 4590, 64-bit processor, and 8 GB of RAM. The average computation times of the developed forecasting framework are 497.882909 s, 415.900852 s, and 492.576224 s for short-term wind speed, electrical power load, and electricity price, respectively. Among all the models, the developed forecasting

framework spends the longest time in computing. However, although it is the most time-consuming model, the time spent is within the acceptable scale and the model achieves the best performance. Overall, this is admissible in practical implementation.

6. Conclusion

To the best knowledge of the authors, the EPS always plays a significant role in economic and social developments. However,

Table 11Comparison of RE_{MAPE} (%) results.

Experiment	ENN vs. GRNN			MODA-ENN vs. ENN			
	1-Step	2-Step	3-Step	1-Step	2-Step	3-Step	
EXP.1	16.980321	10.345254	7.458706	8.149516	7.954064	8.503438	
EXP.2	23.178110	16.878539	19.683629	5.866388	6.823079	4.446383	
EXP.3	25.039354	14.630645	16.427931	3.342699	5.308012	6.525452	
MODA-ENN vs. PSO-ENN							
1-Step	2-Step	3-Step	1-Step	2-Step	3-Step		
EXP.1	5.017772	3.090853	2.319983	56.241299	44.184726	32.284508	
EXP.2	1.776508	4.480627	2.325289	51.493770	42.424415	32.565907	
EXP.3	2.423079	2.620795	5.046499	52.631750	42.875850	24.327374	
ICEEMDAN-ENN vs. EMD-ENN							
1-Step	2-Step	3-Step	1-Step	2-Step	3-Step		
EXP.1	24.378335	11.993515	4.388110	14.482827	7.739287	5.788296	
EXP.2	17.361903	10.689789	17.126448	10.634988	8.426787	8.700953	
EXP.3	33.793517	26.260416	17.812729	9.511040	4.596860	8.238142	
ICEEMDAN-MODA-ENN vs. MODA-ENN							
1-Step	2-Step	3-Step	1-Step	2-Step	3-Step		
EXP.1	57.185829	45.376276	33.246805	10.125519	9.913425	9.775300	
EXP.2	56.033558	44.998612	34.435702	14.752264	10.988575	7.028865	
EXP.3	53.946916	44.596285	23.655500	5.657315	7.669361	5.590882	
ICEEMDAN-MODA-ENN vs. ICEEMDAN-ENN							
1-Step	2-Step	3-Step	1-Step	2-Step	3-Step		

although previous studies are relevant, these leave much for improvement as they do not always meet growing management requirements significant for EPS and even for the entire national economic and social developments. More serious than the aforementioned, most previous researches are focused on accuracy improvements and usually ignore the significance of forecasting stability. Therefore, developing an effective and robust forecasting framework for EPS as well improving forecasting performance become highly desirable. In this paper, to overcome the deficiencies discussed above, a hybrid forecasting framework consisting of four modules—data preprocessing, optimization, forecasting, and evaluation modules—was successfully developed by the authors. First, to boost forecasting effectiveness, the original time series in the EPS are decomposed and reconstructed using the advanced decomposition approach in the data preprocessing module. Second, to simultaneously achieve high accuracy and stability, the ENN model optimized by the multi-objective optimization algorithm is employed to forecast future changes in the forecasting module. Third, multi-step forecasting is conducted for the EPS and finally, the evaluation module is employed to perform comprehensive evaluation and verify the effectiveness of the hybrid forecasting framework.

In this framework, the significance of the data preprocessing module is that the main features of the data in EPS can be effectively extracted and identified. This resulted in 56.713564%, 53.763664%, and 53.289333% reductions in MAPE compared to those of the comparison models in one-step wind speed forecasting, electrical power load forecasting, and electricity price forecasting, respectively. On the other hand, the optimization module resulted in 9.137517%, 10.309326%, and 4.500007% reductions in MAPE in one-step forecasting for wind speed, electrical power load, and electricity price, respectively. These reductions demonstrate the significance of the module to overcome the drawbacks of previous work using single-objective optimization

Table 13
Comparison results of the computational times.

Model	Time (s)	Model	Time (s)
Short-term wind speed time series			
ENN	33.650660	EEMD-ENN	121.512163
GRNN	45.799067	MODA-ENN	396.758615
PSO-ENN	335.157462	ICEEMDAN-ENN	203.791466
EMD-ENN	32.480579	ICEEMDAN-MODA-ENN	497.882909
Electrical load time series			
ENN	8.361355	EEMD-ENN	30.840506
GRNN	2.348041	MODA-ENN	382.475156
PSO-ENN	277.077842	ICEEMDAN-ENN	52.688242
EMD-ENN	8.420606	ICEEMDAN-MODA-ENN	415.900852
Electricity price time series			
ENN	12.798870	EEMD-ENN	58.445578
GRNN	7.241332	MODA-ENN	414.950408
PSO-ENN	294.433130	ICEEMDAN-ENN	84.152303
EMD-ENN	12.644865	ICEEMDAN-MODA-ENN	492.576224

algorithm. The forecasting module can therefore provide basic information for scientific operations of the EPS and market participants. Furthermore, the comprehensive evaluation module is an integral part of a complete forecasting framework. From a series of experimental results, the developed hybrid forecasting framework for one step forecasting led to 44.271386%, 43.967988%, and 44.271386% reductions in MAPE compared to the comparison models in short-term wind speed forecasting, electrical power load forecasting, and electricity price forecasting, respectively. As for three-step forecasting in wind speed, electrical power load, and electricity price, reductions in MAPE are 26.987216%, 28.908219%, and 26.987216%, respectively. In general, the most important significance of the developed forecasting framework is to perform multi-step forecasting for complex and crucial EPS instead of the

Table 12
Comparison of results of the forecasting steps.

Metric	One-Step	Two-Step	Improvement	Three-Step	Improvement
Short-term wind speed time series					
AE (m/s)	0.011228	0.024395	0.013167	0.042681	0.031453
MAE (m/s)	0.168734	0.265621	0.096887	0.364905	0.196171
RMSE (m/s)	0.233978	0.379505	0.145528	0.543285	0.309308
NMSE (–)	0.001180	0.002989	0.001809	0.006215	0.005034
MAPE (%)	3.112065	4.959388	1.847322	6.826262	3.714196
IA (–)	0.997573	0.993591	0.003982	0.986820	0.010752
FB (–)	-0.001906	-0.004135	0.002229	-0.007216	0.005310
TIC (–)	0.018258	0.029546	0.011288	0.042157	0.023899
Electrical load time series					
AE (MW)	4.030220	7.573474	3.543254	11.855555	7.825335
MAE (MW)	28.455481	48.760478	20.304997	69.585411	41.129930
RMSE (MW)	38.090754	67.325803	29.235048	102.613956	64.523202
NMSE (–)	0.000022	0.000072	0.000049	0.000168	0.000146
MAPE (%)	0.380740	0.648364	0.267625	0.917687	0.536948
IA (–)	0.999566	0.998693	0.000874	0.996895	0.002672
FB (–)	-0.000510	-0.000954	0.000444	-0.001485	0.000975
TIC (–)	0.002472	0.004343	0.001872	0.006632	0.004160
Electricity price time series					
AE (\$MWh)	0.444801	0.641239	0.196438	0.702883	0.258082
MAE (\$MWh)	1.896813	2.700568	0.803755	3.472515	1.575702
RMSE (\$MWh)	4.805278	5.892429	1.087151	6.634617	1.829339
NMSE (–)	0.005568	0.008052	0.002484	0.008332	0.002763
MAPE (%)	1.477707	2.189505	0.711798	3.032875	1.555168
IA (–)	0.982066	0.970169	0.011897	0.948501	0.033565
FB (–)	-0.003334	-0.004581	0.001247	-0.005037	0.001703
TIC (–)	0.019900	0.024860	0.004960	0.029547	0.009647

(–) indicates without measurement unit.

single signals in EPS. With high forecasting accuracy and stability, the framework can bring enormous benefits in electrical power scheduling and provide the basic information for decision-makers. Based on the above comparative studies and discussions, the developed hybrid forecasting framework has been proven excellent in many respects compared with other models. This indicate that each of its component is promising and effective for improving forecasting performance. Moreover, based on the DM test and FE values, it can be reasonably concluded that the degree of forecasting accuracy of the developed forecasting framework is higher than and significantly different from those of benchmark models. In summary, the combination and full use of the strengths and advantages of each component of the hybrid network ultimately contributed to its final success rendering it effective for application in the EPS or other fields of engineering in the future.

Conflicts of interest

The authors declare that there is no conflict of interest regarding the publication of this paper.

Acknowledgements

This work was supported by the National Natural Science Foundation of China (grant number 71671029).

References

- [1] Wang J, Hu J, Ma K, Zhang Y. A self-adaptive hybrid approach for wind speed forecasting. *Renew Energy* 2015;78:374–85. <https://doi.org/10.1016/j.renene.2014.12.074>.
- [2] Ou TC, Hong CM. Dynamic operation and control of microgrid hybrid power systems. *Energy* 2014;66:314–23. <https://doi.org/10.1016/j.energy.2014.01.042>.
- [3] Ou TC, Su WF, Liu XZ, et al. A modified Bird-Mating optimization with Hill-Climbing for connection decisions of transformers. *Energies* 2016;9(9). <https://doi.org/10.3390/en9090671>.
- [4] Liu Y, Wang W, Ghadimi N. Electricity load forecasting by an improved forecast engine for building level consumers. *Energy* 2017;139:18–30. <https://doi.org/10.1016/j.energy.2017.07.150>.
- [5] Yuan X, Tan Q, Lei X, Yuan Y, Wu X. Wind power prediction using hybrid autoregressive fractionally integrated moving average and least square support vector machine. *Energy* 2017;129:122–37. <https://doi.org/10.1016/j.energy.2017.04.094>.
- [6] Ambach D, Schmid W. A new high-dimensional time series approach for wind speed, wind direction and air pressure forecasting. *Energy* 2017;135:833–50. <https://doi.org/10.1016/j.energy.2017.06.137>.
- [7] Jiang H, Dong Y. Global horizontal radiation forecast using forward regression on a quadratic kernel support vector machine: case study of the Tibet autonomous region in China. *Energy* 2017;133:270–83. <https://doi.org/10.1016/j.energy.2017.05.124>.
- [8] Paulescu M, Brabec M, Boata R, Badescu V. Structured, physically inspired (gray box) models versus black box modeling for forecasting the output power of photovoltaic plants. *Energy* 2017;121:792–802. <https://doi.org/10.1016/j.energy.2017.01.015>.
- [9] Ou TC. A novel unsymmetrical faults analysis for microgrid distribution systems. *Int J Electr Power Energy Syst* 2012;43:1017–24. <https://doi.org/10.1016/j.ijepes.2012.05.012>.
- [10] Ou TC. Ground fault current analysis with a direct building algorithm for microgrid distribution. *Int J Electr Power Energy Syst* 2013;53:867–75. <https://doi.org/10.1016/j.ijepes.2013.06.005>.
- [11] Lin WM, Ou TC. Unbalanced distribution network fault analysis with hybrid compensation. *IET Gener Transm Distrib* 2010;5(1):92–100. <https://doi.org/10.1049/iet-gtd.2008.0627>.
- [12] Ou TC, Lu KH, Huang CJ. Improvement of transient stability in a hybrid power multi-system using a designed NIDC (novel intelligent damping controller). *Energies* 2017;10(4):488. <https://doi.org/10.3390/en10040488>.
- [13] Jiang P, Ma X. A hybrid forecasting approach applied in the electrical power system based on data preprocessing, optimization and artificial intelligence algorithms. *Appl Math Model* 2016;40:10631–49. <https://doi.org/10.1016/j.apm.2016.08.001>.
- [14] Georgilakis PS. Technical challenges associated with the integration of wind power into power systems. *Renew Sustain Energy Rev* 2008;12:852–63. <https://doi.org/10.1016/j.rser.2006.10.007>.
- [15] Global Wind Energy Council. China Wind Power Blows Past EU. Available online: <http://myemail.constantcontact.com/China-Wind-Power-Blows-Past-EU.html?sid=1102949362881&aid=x4fuGfjtXU> (Accessed 10 February 2016).
- [16] Zhang C, Wei H, Zhao X, Liu T, Zhang KA. Gaussian process regression based hybrid approach for short-term wind speed prediction. *Energy Convers Manag* 2016;126:1084–92. <https://doi.org/10.1016/j.enconman.2016.08.086>.
- [17] Jung J, Broadwater RP. Current status and future advances for wind speed and power forecasting. *Renew Sustain Energy Rev* 2014;31:762–77. <https://doi.org/10.1016/j.rser.2013.12.054>.
- [18] Liu Z, Wang D, Jia H, Djilali N. Power system operation risk analysis considering charging load self-management of plug-in hybrid electric vehicles. *Appl Energy* 2014;136:662–70. <https://doi.org/10.1016/j.apenergy.2014.09.069>.
- [19] Yang W, Wang J, Wang R. Research and application of a novel hybrid model based on data selection and artificial intelligence algorithm for short term load forecasting. *Entropy* 2017. <https://doi.org/10.3390/e19020052>.
- [20] Wang D, Luo H, Grunder O, Lin Y, Guo H. Multi-step ahead electricity price forecasting using a hybrid model based on two-layer decomposition technique and BP neural network optimized by firefly algorithm. *Appl Energy* 2017;190:390–407. <https://doi.org/10.1016/j.apenergy.2016.12.134>.
- [21] Shu F, Luonan C. Short-term load forecasting based on an adaptive hybrid method. *Power Syst IEEE Trans* 2006;21:392–401. <https://doi.org/10.1109/TPWRS.2005.860944>.
- [22] Liu H, Tian H, Liang X, Li Y. Wind speed forecasting approach using secondary decomposition algorithm and Elman neural networks. *Appl Energy* 2015;157:183–94. <https://doi.org/10.1016/j.apenergy.2015.08.014>.
- [23] Raza MQ, Khosravi A. A review on artificial intelligence based load demand forecasting techniques for smart grid and buildings. *Renew Sustain Energy Rev* 2015;50:1352–72. <https://doi.org/10.1016/j.rser.2015.04.065>.
- [24] Lee CM, Ko CN. Short-term load forecasting using lifting scheme and ARIMA models. *Expert Syst Appl* 2011;38:5902–11. <https://doi.org/10.1016/j.eswa.2010.11.033>.
- [25] Cadenas E, Rivera W. Wind speed forecasting in three different regions of Mexico, using a hybrid ARIMA-ANN model. *Renew Energy* 2010;35:2732–8. <https://doi.org/10.1016/j.renene.2010.04.022>.
- [26] Wang Y, Wang J, Zhao G, Dong Y. Application of residual modification approach in seasonal ARIMA for electricity demand forecasting: a case study of China. *Energy Pol* 2012;48:284–94. <https://doi.org/10.1016/j.enpol.2012.05.026>.
- [27] Contreras J, Espinola R, Nogales FJ, Conejo AJ. ARIMA models to predict next-day electricity prices. *IEEE Trans Power Syst* 2003;(18):1014–20. <https://doi.org/10.1109/TPWRS.2002.804943>.
- [28] Lynch C, OMahony MJ, Scully T. Simplified method to derive the Kalman Filter covariance matrices to predict wind speeds from a NWP model. *Energy Procedia* 2014;62:676–85. <https://doi.org/10.1016/j.egypro.2014.12.431>.
- [29] De Felice M, Alessandri A, Ruti PM. Electricity demand forecasting over Italy: potential benefits using numerical weather prediction models. *Elec Power Syst Res* 2013;104:71–9. <https://doi.org/10.1016/j.epsr.2013.06.004>.
- [30] De Giorgi MG, Fiarella A, Tarantino M. Assessment of the benefits of numerical weather predictions in wind power forecasting based on statistical methods. *Energy* 2011;36:3968–78. <https://doi.org/10.1016/j.energy.2011.05.006>.
- [31] Zhang J, Draxl C, Hopson T, Monache LD, Vanvyve E, Hodge BM. Comparison of numerical weather prediction based deterministic and probabilistic wind resource assessment methods. *Appl Energy* 2015;156:528–41. <https://doi.org/10.1016/j.apenergy.2015.07.059>.
- [32] Hong WC. Electric load forecasting by seasonal recurrent SVR (support vector regression) with chaotic artificial bee colony algorithm. *Energy* 2011;36:5568–78. <https://doi.org/10.1016/j.energy.2011.07.015>.
- [33] Lou CW, Dong MC. A novel random fuzzy neural networks for tackling uncertainties of electric load forecasting. *Int J Electr Power Energy Syst* 2015;73:34–44. <https://doi.org/10.1016/j.ijepes.2015.03.003>.
- [34] Guo Z, Zhao J, Zhang W, Wang J. A corrected hybrid approach for wind speed prediction in Hexi Corridor of China. *Energy* 2011;36:1668–79. <https://doi.org/10.1016/j.energy.2010.12.063>.
- [35] Niu T, Wang J, Zhang K, Du P. Multi-step-ahead wind speed forecasting based on optimal feature selection and a modified Bat algorithm with the cognition strategy. *Renew Energy* 2017. <https://doi.org/10.1016/j.renene.2017.10.075>.
- [36] Panapakidis IP, Dagoumas AS. Day-ahead electricity price forecasting via the application of artificial neural network based models. *Appl Energy* 2016;172:132–51. <https://doi.org/10.1016/j.apenergy.2016.03.089>.
- [37] Jiang H, Wang J, Dong Y, Lu H. Comprehensive assessment of wind resources and the low-carbon economy: an empirical study in the Alxa and Xilin Gol Leagues of inner Mongolia, China. *Renew Sustain Energy Rev* 2015;50:1304–19. <https://doi.org/10.1016/j.rser.2015.05.082>.
- [38] Geng Z, Yang X, Han Y, Zhu Q. Energy optimization and analysis modeling based on extreme learning machine integrated index decomposition analysis: application to complex chemical processes. *Energy* 2017;120:67–78. <https://doi.org/10.1016/j.energy.2016.12.090>.
- [39] Kusumo F, Silitonga AS, Masjuki HH, Ong HC, Siswantoro J, Mahlia TMI. Optimization of transesterification process for Ceiba pentandra oil: a comparative study between kernel-based extreme learning machine and artificial neural networks. *Energy* 2017;134:24–34. <https://doi.org/10.1016/j.energy.2017.05.196>.
- [40] Li J, Wang R, Wang J, Li Y. Analysis and forecasting of the oil consumption in China based on combination models optimized by artificial intelligence algorithms. *Energy* 2018;144:243–64. <https://doi.org/10.1016/j.energy.2018.03.090>.

- j.energy.2017.12.042.
- [41] Metaxiotis K, Kagiannas A, Askounis D, Psarras J. Artificial intelligence in short term electric load forecasting: a state-of-the-art survey for the researcher. *Energy Convers Manag* 2003;44:1525–34. [https://doi.org/10.1016/S0196-8904\(02\)00148-6](https://doi.org/10.1016/S0196-8904(02)00148-6).
- [42] Li P, Li Y, Xiong Q, Chai Y, Zhang Y. Application of a hybrid quantized Elman neural network in short-term load forecasting. *Int J Electr Power Energy Syst* 2014;55:749–59. <https://doi.org/10.1016/j.ijepes.2013.10.020>.
- [43] Jiang P, Wang Y, Wang J. Short-term wind speed forecasting using a hybrid model. *Energy* 2017;119:561–77. <https://doi.org/10.1016/j.energy.2016.10.040>.
- [44] Wang J, Hu J. A robust combination approach for short-term wind speed forecasting and analysis - combination of the ARIMA (autoregressive integrated moving average), ELM (extreme learning machine), SVM (support vector machine) and LSSVM (least square SVM) forecasts using a GPR (Gaussian process regression) model. *Energy* 2015;93:41–56. <https://doi.org/10.1016/j.energy.2015.08.045>.
- [45] Jiang P, Liu F, Song Y. A hybrid forecasting model based on date-framework strategy and improved feature selection technology for short-term load forecasting. *Energy* 2017;119:694–709. <https://doi.org/10.1016/j.energy.2016.11.034>.
- [46] Yang Y, Che J, Li Y, Zhao Y, Zhu S. An incremental electric load forecasting model based on support vector regression. *Energy* 2016;113:796–808. <https://doi.org/10.1016/j.energy.2016.07.092>.
- [47] Yang Z, Ce L, Lian L. Electricity price forecasting by a hybrid model, combining wavelet transform, ARMA and kernel-based extreme learning machine methods. *Appl Energy* 2017;190:291–305. <https://doi.org/10.1016/j.apenergy.2016.12.130>.
- [48] Singh N, Mohanty SR, Dev Shukla R. Short term electricity price forecast based on environmentally adapted generalized neuron. *Energy* 2017;125:127–39. <https://doi.org/10.1016/j.energy.2017.02.094>.
- [49] Juang C-F. A hybrid of genetic algorithm and particle swarm optimization for recurrent network design. *IEEE Trans Syst Man Cybern B Cybern* 2004;(34): 997–1006. <https://doi.org/10.1109/TSMCB.2003.818557>.
- [50] Velázquez S, Carta JA, Matías JM. Influence of the input layer signals of ANNs on wind power estimation for a target site: a case study. *Renew Sustain Energy Rev* 2011;15:1556–66. <https://doi.org/10.1016/j.rser.2010.11.036>.
- [51] Ma X, Jin Y, Dong Q. A generalized dynamic fuzzy neural network based on singular spectrum analysis optimized by brain storm optimization for short-term wind speed forecasting. *Appl Soft Comput* 2017;54:296–312. <https://doi.org/10.1016/j.asoc.2017.01.033>.
- [52] Xiao L, Shao W, Wang C, Zhang K, Lu H. Research and application of a hybrid model based on multi-objective optimization for electrical load forecasting. *Appl Energy* 2016;180:213–33. <https://doi.org/10.1016/j.apenergy.2016.07.113>.
- [53] Colominas MA, Schlotthauer G, Torres ME. Improved complete ensemble EMD: a suitable tool for biomedical signal processing. *Biomed Signal Process Contr* 2014;14:19–29. <https://doi.org/10.1016/j.bspc.2014.06.009>.
- [54] Huang NE, Shen Z, Long SR, Wu MC, Shih HH, Yen N, et al. The empirical mode decomposition and the Hilbert spectrum for nonlinear and non-stationary time series analysis. *R Soc London Proc Ser A* 1996;454. <https://doi.org/10.1098/rspa.1998.0193>. 903–95.
- [55] Flandrin P, Rilling G, Goncalves P. Empirical mode decomposition as a filter bank. *IEEE Signal Process Lett* 2004;(11):112–4. <https://doi.org/10.1109/LSP.2003.821662>.
- [56] Wu Z, Huang NE. Ensemble empirical mode decomposition. *Adv Adapt Data Anal* 2009;(1):1–41. <https://doi.org/10.1515/BMT.2010.030>.
- [57] Torres ME, Colominas MA, Schlotthauer G, Flandrin P. A complete ensemble empirical mode decomposition with adaptive noise. In: ICASSP, IEEE International Conference on Acoustics, Speech and Signal Processing - Proceedings; 2011. p. 4144–7. <https://doi.org/10.1109/ICASSP.2011.5947265>.
- [58] Mirjalili S. Dragonfly algorithm: a new meta-heuristic optimization technique for solving single-objective, discrete, and multi-objective problems. *Neural Comput Appl* 2016;27:1053–73. <https://doi.org/10.1007/s00521-015-1920-1>.
- [59] Sree RKS, Murugan S. Memory based hybrid dragonfly algorithm for numerical optimization problems. *Expert Syst Appl* 2017;83. <https://doi.org/10.1016/j.eswa.2017.04.033>.
- [60] Mirjalili S, Lewis A. Novel performance metrics for robust multi-objective optimization algorithms. *Swarm Evol Comput* 2015;21:1–23. <https://doi.org/10.1016/j.swevo.2014.10.005>.
- [61] Coello CAC. Evolutionary multi-objective optimization: some current research trends and topics that remain to be explored. *Front Comput Sci China* 2009;3: 18–30. <https://doi.org/10.1007/s11704-009-0005-7>.
- [62] Ngatchou P, Zarei A, El-Sharkawi A. Pareto multi objective optimization. In: Proc 13th Int Conf on, Intell Syst Appl to power Syst; 2005. p. 84–91. <https://doi.org/10.1109/ISAP.2005.1599245>.
- [63] Coello CAC, Lechuga MS. MOPSO: a proposal for multiple objective particle swarm optimization. In: Proc. 2002 Congr. Evol. Comput. Cec 2002, vol. 2; 2002. p. 1051–6. <https://doi.org/10.1109/CEC.2002.1004388>.
- [64] Coello CAC, Pulido GT, Lechuga MS. Handling multiple objectives with particle swarm optimization. *Evol Comput IEEE Trans* 2004;(8):256–79. <https://doi.org/10.1109/TEVC.2004.826067>.
- [65] Elman JL. Finding structure in time. *Cognit Sci* 1990;14:179–211. [https://doi.org/10.1016/0364-0213\(90\)90002-E](https://doi.org/10.1016/0364-0213(90)90002-E).
- [66] Xu Y, Du P, Wang J. Research and application of a hybrid model based on dynamic fuzzy synthetic evaluation for establishing air quality forecasting and early warning system: a case study in China. *Environ Pollut* 2017. <https://doi.org/10.1016/j.envpol.2017.01.043>.
- [67] Hong CM, Ou TC, Lu KH. Development of intelligent MPPT (maximum power point tracking) control for a grid-connected hybrid power generation system. *Energy* 2013;50:270–9. <https://doi.org/10.1016/j.energy.2012.12.017>.
- [68] Lin WM, Hong CM, Huang CH, Ou TC. Hybrid control of a wind induction generator based on grey-Elman neural network. *IEEE Trans Contr Syst Technol* 2013;(21):2367–73. <https://doi.org/10.1109/TCS.2012.2231865>.
- [69] Wang J, Du P, Niu T, Yang W. A novel hybrid system based on a new proposed algorithm-Multi-Objective Whale Optimization Algorithm for wind speed forecasting. *Appl Energy* 2017. <https://doi.org/10.1016/j.apenergy.2017.10.031>.
- [70] Du P, Wang J, Guo Z, Yang W. Research and application of a novel hybrid forecasting system based on multi-objective optimization for wind speed forecasting. *Energy Convers Manag* 2017;150. <https://doi.org/10.1016/j.enconman.2017.07.065>.
- [71] Wang J, Heng J, Xiao L, Wang C. Research and application of a combined model based on multi-objective optimization for multi-step ahead wind speed forecasting. *Energy* 2017. <https://doi.org/10.1016/j.energy.2017.02.150>.
- [72] Xu Y, Yang W, Wang J. Air quality early-warning system for cities in China. *Atmos Environ* 2017. <https://doi.org/10.1016/j.atmosenv.2016.10.046>.
- [73] Diebold FX, Mariano RS. Comparing predictive accuracy. *J Bus Econ Stat* 1995;13:253–65. <https://doi.org/10.1080/07350015.1995.10524599>.
- [74] Chen H, Hou D. Research on superior combination forecasting model based on forecasting effective measure. *J. Univ. Sci. Technol. China* 2002;2:172–80.